# REVISION #2.

# A Rock Fragment Related to the Magnesian Suite in Lunar Meteorite Allan Hills (ALHA) A81005

Allan H. Treiman[1], and Juliane Gross[2].

[1] Lunar and Planetary Institute, 3600 Bay Area Boulevard, Houston TX 77058-1113. treiman@lpi.usra.edu

[2] Department of Earth and Planetary Sciences, American Museum of Natural History, Central Park West at 79th Street, New York NY 10024.

## ABSTRACT

Among the lunar samples that were returned by the Apollo missions are many cumulate plutonic rocks with high Mg# (molar Mg/(Mg+Fe) in %) and abundances of KREEP elements (Potassium, Rare Earth Elements, Phosphorus, U, Th, etc.) that imply KREEP-rich parental magmas. These rocks, collectively called the magnesian suite, are nearly absent from sampling sites distant from Imbrium basin ejecta, including those of lunar highlands meteorites. This absence has significant implications for the early differentiation of the Moon and its distribution of heat-producing elements (K, Th, U). Here, we analyze a unique fragment of basalt with the mineralogy and mineral chemistry of a magnesian suite rock, in the lunar highlands meteorite Allan Hills (ALH) A81005. In thin section, the fragment is 700 x 300 µm, and has a sub-ophitic texture with olivine phenocrysts, euhedral plagioclase grains (An97-90), and interstitial pyroxenes. Its minerals are chemically equilibrated. Olivine has Fe/Mn ~ 70 (consistent with a lunar origin), and Mg# ~80, which is consistent with rocks of the magnesian suite and far higher than in mare basalts. It has a rich suite of minor minerals: fluorapatite, ilmenite, Zr-armalcolite, chromite, troilite, silica, & Fe metal (Ni=3.8%, Co=0.17%). The metal is comparable to that in chondrite meteorites, which suggests that the fragment is from an impact melt. The fragment itself is not a piece of magnesian suite rock (which are plutonic), but its mineralogy and mineral chemistry suggest that its protolith (which was melted by impact) was related to the magnesian suite. However, the fragment's mineral chemistry and minor minerals are not identical to those of known magnesian suite rocks, suggesting that the suite may be more varied than apparent in the Apollo samples. Although ALHA81005 is from the lunar highlands (and likely from the farside), Clast U need not have formed in the highlands. It could have formed in an impact melt pool on the nearside and been transported by meteoroid impact. Lunar highlands meteorites should be searched for rock fragments related to the magnesian-suite rocks, but the fragments are rare and may have mineral compositions similar to some meteoritic (impactor) materials.

Key words: ALHA 81005, Moon, lunar, petrology, 'magnesian suite,' armalcolite, 'impact melt,' 'lunar meteorite.'

## INTRODUCTION

Among the samples returned from the Apollo landing sites are many fragments of magnesian plutonic rocks: norites, gabbros, troctolites, and dunites. These rocks are distinct from mare basalts (and their kin) in being far more magnesian [with higher Mg# = molar Mg/(Mg+Fe) in %], and distinct from lunar ferroan anorthosites in being more magnesian and containing much less plagioclase. These plutonic rocks are considered to be a broadly-related group, the 'magnesian suite,' derived from Mg-rich basaltic magmas that were enriched in igneous incompatible elements, the KREEP component (Fig. 1; James and Flohr 1983; Norman and Ryder 1980; Shearer and Papike 2005; Elardo et al. 2011). In the canonical view of lunar petrology, magnesian suite magmas post-date formation of the lunar crust from the magma ocean, solidification of the magma ocean with formation of the KREEP component as its last fractionate, and gravitational overturn of the lunar mantle (Snyder et al. 1995; Shearer and Papike 1999; McCallum and Schwarz 2001; Shearer et al. 2006; Wieczorec et al. 2006; Elkins-Tanton et al. 2011). The chemistry of the magnesian suite suggests that its sources formed as mixtures of KREEP and early magnesian cumulates from the magma ocean, mixed during the overturn of the Moon's mantle, and perhaps brought to partial melting by heat generated in the overturn. Magnesian suite magmas intruded the anorthosite crust as layered basic intrusions, and our samples of magnesian suite rock are fragments excavated (by impact) from those intrusions. This model does present some problems of chronology and geochemistry (Elkins-Tanton et al. 2011; Gross et al. 2014), but suffices here as a broad geological background.

Rocks of the Stillwater complex, a large layered basaltic intrusion (McCallum 1996), have played a significant role in interpretation of lunar magnesian suite samples. Recognition that the lunar crust was anorthositic (Wood et al. 1970) brought attention to terrestrial analogs. The Stillwater complex was prominent among the analogs because it includes thick layers of massive anorthosite, was accessible to geologists in North America, and was being intensely studied for its economic potential. The close similarities of mineral composition trends in the Stillwater to those in lunar highland samples (Raedeke and McCallum 1980), suggested that the Moon could be viewed as a series of overlapping layered basic intrusions. Although that model is not in the canonical picture of the Moon, the similarity remains and informs our understanding of lunar crustal processes.

In the years since the First Conference on the Lunar Highlands, in 1980, lunar meteorites have greatly expanded our understanding of the lunar surface. Approximately 75 distinct lunar meteorites are now known, nearly all of which are regolith breccias full of rock fragments (Korotev 2014). The lunar meteorites appear to represent a random sampling of sites across the whole lunar surface, mare and feldspathic highlands, with most hailing from regions outside those sampled by Apollo and Luna missions (Korotev 2005). Feldspathic meteorites from areas near the Apollo landing sites are recognized by their similarity to returned samples: abundant clasts of ferroan anorthosite, some clasts of magnesian-suite rock, and KREEPy bulk compositions. Such meteorites include Y983885 (Arai et al. 2005), NWA5406 (Korotev et al. 2009), and MIL090034 (Liu et al. 2011).

The majority of feldspathic meteorites are distinct from returned samples in having abundant clasts of magnesian granulites and anorthosites, rare clasts of ferroan anorthosite, and nearly no clasts of magnesian-suite rock (Gross et al. 2014). Bulk compositions of these feldspathic meteorites are magnesian (Mg# of ~75; see Fig. 1), and contain very low abundances of KREEP elements (Korotev et al. 2003, 2006, 2012); these characteristics are consistent with orbital chemical data for the lunar highlands (Jolliff et al. 2000), and are most consistent with origins in the lunar farside highlands (Pieters et al. 1983; Kallemeyn and Warren 1983; Korotev et al. 1983; Isaacson et al. 2013). The granulites and anorthosites in farside feldspathic meteorites have mineral compositions (An in plagioclase, Mg# in olivine and pyroxenes) that are consistent the magnesian suite (Fig. 1), but their minor- and trace-element chemistries suggest a different origin (Korotev et al. 2003; Treiman et al. 2010).

Clasts of magnesian suite rock are nearly absent from these feldspathic lunar meteorites (e.g., Jolliff et al. 1991; Daubar et al. 2002; Korotev et al. 2003; Cahill et al. 2004; Korotev 2005; Sokol et al. 2008; Snape et al. 2011; Gross et al. 2014). Only a few clasts or groups of clasts with mineralogy and mineral chemistry that could be ascribed to the magnesian suite have been reported, and none is documented in detail. [1] In meteorite ALHA81005 (thin section ,9), Treiman and Drake (1983) ascribed their clast U to the magnesian suite based on the compositions of plagioclase and mafic minerals, and the presence of Zr-bearing armalcolite (Treiman and Gross 2013). [2] In the Calcalong Creek meteorite, Marvin and Holmberg (1992) reported a clast of partially remelted spinel troctolite with olivine of $Fo_{90-92}$. [3] In the Dhofar 305 and 307 meteorites (paired with Dhofar 489, 309, and others), Demidova et al. (2003) reported clasts with An of 88-92 and Mg# of ~75, which are consistent with a magnesian suite parentage. No additional data are available. [4] In Dhofar 025, Cahill et al. (2004) reported that a rock fragment (# 25.8) contains plagioclase of ~$An_{91}$ and mafics (olivine, low-Ca pyroxene) with Mg# of ~89. These mineral compositions place the clast near the magnesian suite field, Figure 1. [5] In meteorite Y86032, Yamaguchi et al. (2010) reported fragments of anorthosite with plagioclase of An91-94 and mafic silicates (olivine, augite, low-Ca pyroxene) with Mg# of 78-85, which are consistent with mineral compositions of the magnesian suite, Figure 1. However, the breccia that hosts these fragments is geochemically distinct from the magnesian suite (as known from Apollo samples) and more characteristic of ferroan anorthosite in being anorthositic, having low abundances of incompatible elements, and having a high Ti/Sm ratio (Yamaguchi et al. 2010).

The rarity of magnesian suite lithologies in feldspathic lunar meteorites presents a geological conundrum. Magnesian suite rocks in the Apollo collection all formed from magmas with significant proportions of the KREEP component: "The KREEP signature, though, seems invariably tied to [magnesian]-suite petrogenesis, as there are no [magnesian]-suite rocks in the sample collection without the KREEP signature that is prevalent in many lithologies from the [Procellarum KREEP terrane]" (Elardo et al. 2011). This association of Apollo magnesian suite rocks with KREEP has led to hypotheses that KREEP is essential for their parent magmas, perhaps through its high abundances of the heat-producing elements K, Th, and U (Shearer and Papike 2005). If this argument holds, the lunar highlands far from the Procellarum KREEP Terrane should be as devoid of magnesian suite rocks as it is of KREEP component (Jolliff et al. 2000; Gillis et al. 2004; Kobayashi et al. 2012), except perhaps within the South Pole – Aitken basin. On the other hand, many rock fragments (granulites and other impactities) in meteorites from the highlands have mineral compositions that are consistent with those of magnesian suite rocks (Fig. 1), but lack a detectable signature from KREEP (e.g., Korotev et al. 2003; Takeda et al. 2006; Treiman et al. 2010). Could these rock fragments represent rocks of the magnesian suite, extensively modified by meteorite impact? Or could they represent mixing with other, as yet uncharacterized, lithologies (Treiman et al. 2010), possibly including magnesian plutonic rocks derived from magmas with little KREEP component (Korotev et al. 2003)? Quoting Elardo et al. (2011): "However, the discovery of low-KREEP Mg-suite rocks from the far side, perhaps from South Pole Aitken Basin sample return, would be an enormous aid in placing constraints on the nature of Mg-suite magmatism, its connection to KREEP, and post-LMO crust building processes, as well as the differentiation and composition of the Moon."

This study documents a single rock fragment, clast U in ALHA81005, that has been ascribed to the magnesian suite (Treiman and Drake 1983; Treiman and Gross 2013). We will test its affinity to the magnesian suite, determine if it is different from magnesian suite rocks of the Apollo collection, and establish criteria for recognition of magnesian suite lithologies and fragments in other lunar meteorites.

## SAMPLE AND METHODS

Clast U is exposed in thin section ALHA81005,9 (Treiman and Drake 1983), which was made available here by the Meteorite Working Group, and the Curator of Antarctic Meteorites, NASA Johnson Space Center. ALHA81005 was the first meteorite to be recognized as coming from the Earth's Moon (Marvin 1983); it is a regolith breccia composed of rock fragments (mostly rich in plagioclase) in a glassy agglutinitic matrix (Fig. 2a; Kurat and Brandstätter 1983; Marvin 1983; Warren et al. 1983). ALHA81005 contains scattered fragments of mare basalts, mostly Very Low Titanium (Treiman and Drake 1983; Robinson et al. 2012), and rare fragments of unusual lithologies (Goodrich et al. 1984, 1985; Gross and Treiman 2011). Chemically, ALHA81005 is rich in plagiophile elements (Al, Ca, Eu), and has a small proportion of a KREEP component (Boynton and Hill 1983; Kallemeyn and Warren 1983; Korotev et al. 1983).

Clast U is a small fragment, ~300 μm by ~600 μm and roughly elliptical in outline (Fig. 2, 3). Its surroundings are typical for the meteorite: other rock and mineral fragments, cemented together by agglutinitic glass. Clast U is too small, and with mineral grains too large, to permit reconstruction of a precise bulk composition (and interpretation thereof; Warren 2012), but its mineralogy and mineral compositions are indicative of its origin.

Clast U was investigated via optical microscopy (Fig. 2), backscattered electron (BSE) imagery (Fig. 3), X-ray element maps, and chemical analyses of its minerals. Quantitative mineral analyses were obtained with the Cameca SX-100 electron microprobes of the ARES Directorate, NASA Johnson Space Center, and the Department of Earth and Planetary Sciences, American Museum of Natural History (AMNH). For both machines, analyses were obtained at electron accelerating potentials of 15kV. Analyses of mafic silicate minerals and oxides were obtained with a focused beam, 20 nA beam current, and count times on peak and backgrounds of 20-60 seconds (Tables 1, 2). Analyses of plagioclase feldspar were obtained with a 10 μm defocussed beam at a current of 10 nA (Table 1). Standards included well-characterized natural and synthetic materials. In each run, secondary standards were analyzed as unknowns to confirm analytical accuracy. Qualitative chemical analyses were obtained by energy dispersive X-ray analysis on these microprobes.

Quantitative analyses for Ni and Co and other minor elements in olivine were obtained independently at the AMNH microprobe, at 15 kV accelerating potential, with a focused electron beam, and beam current of 100 nA. Count times on peak (and total background) as follows: Ni and Co, 240 sec; Al and Ca, 180 sec; Ti and Cr, 120 sec; and Mn, 90 sec. Standards were as above for the AMNH, Table 3. The lower background position for the CoK$\alpha$ X-rays overlaps slightly with the FeK$\beta$ X-ray peak; the Cameca analysis software corrected for this overlap. We collected 17 individual analyses across three separate olivine grains. Under these conditions, each individual analysis has 3$\sigma$ detection limits for Ni and Co of ~40 ppm. Individual analyses for Co range from <0 to 25 ppm, and so are all below detection. Individual analyses for Ni range from 10 to 90 ppm, and the uncertainty on each from counting statistics is ~6 ppm (2$\sigma$). The population of 17 Ni analyses (Table 3) has a median value of 53 ppm and a mean of 51±33 ppm (2σ).

This mean value represents the sum of all 17 analyses (i.e., a total duration on peak of 4080 seconds), and a total of 9867 counts of ‘peak minus background’. This summed analysis would have a 3σ detection limit (counting statistics) of ~10 ppm Ni. We accept the Ni abundance from the sum of analyses (and its lower detection limit), because it seems reasonable that the 17 individual analyses represent a statistical distribution around a single value. First, it is likely that Ni abundances in the olivines have been homogenized by diffusion. Diffusion coefficients for Ni in olivine are nearly identical to those of Fe, Mg, and Mn (e.g., Petry et al. 2004; Qian et al. 2010; Chakraborty 2010), so that homogeneity in the latter three elements would suggest homogeneity in Ni. Abundances of MgO, FeO, and MnO are essentially constant (Table 3) at 43.2±1.3%, 16.0±0.7% and 0.22±0.02% (2σ). Similarly, the Mg# of the olivine, molar Mg/(Mg+Fe), is also constant at 83±1% (Table 3). Thus, it seems likely that Ni has been homogenized by diffusion, as were Mg, Fe, and Mn. Second, the 17 individual Ni abundances are consistent with a random distribution about a single value, because the mean and median of the population are essentially identical (see above), and because the distribution of Ni abundances approximates a Gaussian curve. The standard error on the average Ni analysis, ±33 ppm (2σ), is larger than the nominal analytical accuracy from counting statistics of ~0.2 ppm (2σ), which could imply that Ni is actually inhomogeneous in the olivine. However, all elements have larger standard errors of the mean than their nominal accuracy from counting statistics; e.g. 0.02% vs 0.003% for MnO. Thus, the difference between the standard error on the population of analyses and their nominal analytical accuracy is inherent to the EMP analyses, and does not suggest that Ni is inhomogeneoustly distributed.

X-ray element maps (Fig. 4) were obtained in wavelength-dispersive mode, with spectrometers tuned to the peaks of K$\alpha$ X-ray emissions for the selected elements (Mg, Si, Al, Ti, Fe, Ca, S, P, Zr, Na, K). X-ray maps were also obtained using the JEOL 5700 FEG-SEM in the ARES Directorate, NASA Johnson Space Center, from energy-dispersive spectra.

Mineral proportions were calculated from X-ray element maps (e.g., Fig. 4) using the multispectral image processing code Multispec© (Biehl and Landgrebe 2002; Lydon 2005; Maloy and Treiman 2007). To obtain abundances of major minerals, it was only necessary to use X-ray maps of Mg, Al, Ca, and Fe. The classification was supervised, with training areas selected manually.

## MINERALOGY & PETROGRAPHY

### Petrography

Clast U is composed of plagioclase, pyroxene, olivine, iron-sulfides, and minor minerals such as apatite, armalcolite, rutile, silica, and FeTi-oxides. Texturally, it is a subophitic basalt – anhedral pyroxene grains fill spaces among euhedral (or subhedral) crystals of plagioclase feldspar (Figs. 3a, 4; Williams et al. 1954). Olivine crystals are anhedral to subhedral (right side of Fig. 4a), contain rare inclusions of plagioclase, and are in contact with plagioclase and pigeonite pyroxene. Olivine is not in contact with augite pyroxene. Conversely, the minor minerals rich in incompatible elements (apatite, armalcolite, rutile, silica) are not associated with olivine, but are concentrated along boundaries between plagioclase and augite (Fig. 4). These textures are consistent with crystallization of a typical basaltic magma, with minerals appearing in the sequence: olivine, plagioclase, pigeonite, augite, and then apatite etc.

These original igneous textures have been disturbed somewhat by shock. All mineral grains are intensely cracked (Figs. 3b, c), and some of its plagioclase has been melted (or annealed) after cracking (Fig. 3b); these effects may be attributed to shock from impacts (e.g., Ostertag 1983). However, there is no evidence that the rock texture has been disturbed by the shock event, i.e. by faulting or brecciation.

**Mineralogy**

**Plagioclase** is the most abundant mineral in Clast U, constituting ~64% of its area in the thin section. The plagioclase is intensely cracked in some areas and uncracked and dense in others (Fig. 3b), which are interpreted to reflect intense shock, partial conversion to maskelynite, and possibly shock-melting. Hence, it was difficult to obtain good chemical analyses by EMP, both from lack of electrical continuity (cracking) and Na loss (amorphization; see Table 1). Most of the plagioclase is An94-97, with a few analyses near An90 (Table 1). X-ray element maps show that the most sodic plagioclase is adjacent to the pyroxene grains and in areas rich in minor minerals.

**Pyroxenes** account for 25% of Clast U, 19% pigeonite and 6% augite (Figs. 3a, 4a; Table 2). The pyroxenes have consistent Mg# of 79-83 (Fig. 5), but vary widely in Ca content from $Wo_{02}$ to $Wo_{40}$; one spot is more calcic at $Wo_{47}$. The zoning is spatially coherent, as seen best in the pyroxene grain at the center of Figure 4a; that pyroxene grades, from the top of Figure 4a downwards, from Ca-poor pigeonite (reddest = richest in Mg) to Ca-rich pigeonite (darker = poorer in Mg) to augite (greenish brown). This zoning is consistent with a fractionation trend from primitive Ca-poor pyroxene to evolved Ca-rich pyroxene. Superimposed on this zoning in the largest pigeonite grain are spots and streaks with higher brightness in BSE, which appear to be exsolutions of high-Ca pyroxene. The brighter spots and streaks become more abundant toward the areas of pure augite. The pyroxene grain at the left edge of the clast in Fig. 3a shows thin stripes brighter and darker in BSE imagery, which may be a lamellar exsolutions of augite and pigeonite. The augite has nearly constant proportions of Ca, Mg, and Fe (Fig. 5). It alternates with lower-Ca pyroxene in a zone at their contacts, which likely represents exsolution lamellae. Cr abundances are identical in all pyroxenes (Fig. 6a). Abundances of Al are constant in each pyroxene species, with augite containing more Al than pigeonite (Fig. 6b). Abundances of Ti increase strongly with Ca content in both pigeonite and augite (Fig. 5c).

**Olivine** accounts for 9% of clast U (Fig. 3a), and is chemically homogeneous at Mg# = 80±2% (Table 1, 3; Fig. 4). The olivines have Fe/Mn ≈ 71, consistent with a lunar origin (Karner et al. 2003). The olivine is also homogeneous in minor element content, with CaO at 0.09 – 0.41% and Ni at 55±33 ppm (2σ). The olivine grains of clast U contain scattered inclusions of plagioclase and possibly chromite towards their edges, but no melt inclusions.

**Minor Minerals** are present in a diverse assemblage, including phosphate, sulfide, metal, and several oxides.

Clast U contains ~0.03% apatite, $Ca_5(PO_4)_3(F,Cl,OH)$, as six small grains embedded in plagioclase and associated with other minor minerals between plagioclase and pyroxene (Fig. 4a). The apatite grains are too small, < 4 μm across, for quantitative analysis (see Goldoff et al. 2012), but are likely to be chlorian fluorapatite based on the relative heights of the FKα and ClKα peaks in energy dispersive X-ray spectra (Figure 7). The hydroxyl content of the apatite is not known. This proportion of apatite implies a bulk P content of ~ 65 ppm, or 0.05 x CI.

Clast U contains five oxide minerals: armalcolite, ilmenite, rutile, chromite, and silica. Armalcolite is present as a few small grains, ~0.02% of the clast, sited between plagioclase and pyroxene crystals. The chemical analysis here (Table 4) differs from that of Treiman and Drake (1983) only in its Fe/Ti ratio. This armalcolite contains significant proportions of Ca and Zr, and thus is of ‘Type 2’ of Haggerty (1973). Its chemical analysis and formula do not charge-balance if all of the Ti is tetravalent (Table 4), which suggests that ~13-23% of the Ti is trivalent (Stanin and Taylor, 1980).

The clast contains several grains of ilmenite, in the same general areas as the armalcolite. The compositions are ~$Ilm_{80}Geik_{15}$ (Table 4), with small proportions of pyrophanite and other components. Rutile was reported by Treiman and Drake (1983) and detected here on X-ray maps, but not analyzed. Clast U includes a few small grains of chromite spinel (Table 4), which contains ~65% $(Mg,Fe)Cr_2O_4$ and ~25% $(Mg,Fe)Al_2O_4$ components. Clast U also contains a single grain of silica, identified by its energy dispersive spectrum, among other minor minerals near one of the augite grains. We have no data on its crystallinity or which polymorph it might be.

Metal and troilite are the dominant opaque phases in Clast U, and together constitute ~0.4% of its area. The metal is principally Fe with 3.8% Ni and 0.17% Co, in agreement with the analyses of Treiman and Drake (1983). The Ni/Co ratio is within uncertainty of the 'cosmic' value of ~20 (Smith and Steele 1976; Papike et al. 1991; Wittmann and Korotev 2013). Troilite is nearly pure FeS, with only 0.2% Ni & 0.02% Co. Analytical totals are from 99.7 to 100%, indicating little or no solid solution toward pyrrhotite, as would be consistent with equilibration with Fe-rich metal.

## DISCUSSION

### Basalt or Impact Melt?

Texturally, clast U is a sub-ophitic basaltic (see above; Fig. 3). To understand its genesis, it is important to know if clast U could be an erupted basalt (reflecting mantle melting and subsequent fractionation), or if it is a basaltic impact melt. Data available here (mineral compositions, mineral proportions, and textures) are not definitive, but suggest that clast U is a fragment of impact melt.

First, the composition of the metal in clast U is consistent with that of chondritic metal, and thus that the clast is impact melt. The Fe metal has Ni and Co in a mass ratio of 22, consistent with the canonical ratio in meteoritic metal (vis. Wittmann and Korotev 2013). However, there is no unique correlation between metal composition and provenance of lunar materials: "As a result of newer data, it is now clear that these earlier boundaries are no longer valid for distinguishing between lunar and meteoroid metal and that there is extensive overlap between the two. If the composition of metal lies within the "meteoritic" field …, this does not imply that it is of meteoroid origin; it may have an indigenous lunar origin. Nor does a composition of Fe metal outside this area mean that it is lunar in origin" (Papike et al. 1991). The metal in clast U is similar to those of erupted Apollo 12 basalts (Papike et al. 1991), but is not similar to that in Apollo Mg-suite rocks (Ryder et al. 1980).

The mineral proportions in clast U are unusual for an erupted basalt, although the clast's proportions may not be representative of a larger rock mass. The clast's ~65% plagioclase is significantly greater than in mare basalts (Taylor et al. 1991) and in most terrestrial basalts, and is similar to that in many recognized impact melts (Vaniman and Papike 1980) consistent with an impact melt origin (e.g., from a plagioclase-rich source rock like a Mg-suite norite or gabbronorite). On the other hand, if its mineral proportions are taken as representative, then Clast U could represent an erupted basalt with excess (accumulated) plagioclase, or as a partially crystallized basalt that lost some late magma (i.e. by 'filter-pressing').

Finally, the mineral texture of clast U is that of a sub-ophitic basalt: equant olivine phenocrysts, abundant plagioclase euhedra, and interstitial pyroxenes. These textures are not typical of impact melts, which commonly contain lithic inclusions, and elongated and/or dendritic crystals of plagioclase, pyroxene, and olivine (Vaniman and Papike 1980). However, clast-free melt rocks with sub-ophtic textures are known as fragments in lunar regolith (e.g., Stöffler et al. 1985); these could have formed in pools of impact melt that cooled slowly enough to develop typical basalt textures. Unfortunately, clast U is too small to apply criteria from crystal size distributions (Fagan et al. 2013), and textures also remain ambiguous.

Thus, it seems likely that Clast U represents an impact melt, as indicated by it mineral and bulk compositions. However, an origin as a true basalt (possibly modified by fractionation of crystals or melt) cannot be excluded.

**Metamorphism**

Whether clast U originated as an impact melt or an erupted basalt, the compositions of its olivine and pyroxenes have been modified significantly by thermal metamorphism. Its olivine is chemically homogeneous (Tables 1,3) in its abundances of Fe, Mg, Mn, Ni, Co, Ca, and Cr.

The pyroxenes of clast U all have the same Fe/Mg ratio, and that ratio is consistent with chemical equilibrium with the olivine (Fig. 5). Abundances of Cr and Al in the pyroxenes vary little, and so appear to have equilibrated (Figs. 6a, b); at least, they are not zoned as one would expect from igneous fractionation. However, Ca in the pyroxenes is strongly zoned in a manner consistent with igneous fractionation from a noritic melt (Fig. 5) – from Ca-poor pigeonite through Ca-rich pigeonite to sub-calcic augite (Figs. 4a, 5). Similarly, Ti abundances in pyroxenes are strongly zoned, and increase monotonically with Ca abundances (Fig. 6c). This zoning could be a relic of original igneous zoning in the pyroxenes.

**Chemical Affinity: Magnesian Suite**

The focus of this work is an understanding the petrologic affinities of Clast U; i.e.

whether it is derived from or representative of a known suite of lunar rocks, like mare basalts, ferroan anorthosites, Mg-suite plutonics, and magnesian feldspathic granulites. Treiman and Drake (1983) suggested that clast U was related to the magnesian suite plutonic rocks because of its major mineral compositions (plagioclase, olivine, pyroxenes), and its suite of minor minerals. The data developed here confirm their conclusions, and permit a detailed documentation of the affinity of clast U to the magnesian suite.

It is clear that Clast U is not related to known mare basalts, even though it may be a basalt itself. Its minerals' compositions (and bulk composition) are far more magnesian than those of mare basalts (Fig. 5), and the olivine in Clast U contains far less Ni and Co than those in mare basalts (Fig. 9). Similarly, Clast U is not related to ferroan anorthosites; it is too magnesian, has too little plagioclase, and its olivine contains too little Co (Fig. 9b).

Clast U does have chemical affinities with lunar magnesian feldspathic granulites, a group of metamorphic rocks with distinctive trace-element compositions (Korotev and Jolliff 2001; Treiman et al. 2010), but cannot be closely related. Clast U is similar to magnesian feldspathic granulites in being: rich in plagioclase, containing olivine and two pyroxenes, and having Mg# s of ~ 78-88 (Table 5; Treiman et al. 2010). The olivine in clast U contains less Ni and Co than olivines in most magnesian feldspathic granulites (Fig. 9), but this dissimilarity is based on data from only four granulite fragments. Abundances of minor minerals (and their trace elements) are more telling, and suggest that clast U is not closely related to the magnesian feldspathic granulites (Table 5). Clast U contains a rich suite of minor minerals, as noted above, which is not seen in the granulites; the few granulites for which data are available contain ~ 1/30 of the proportion of phosphate mineral in clast U, and are not reported to contain minerals with abundant Zr, like the armalcolite here (Treiman et al. 2010).

On the other hand, clast U's mineral proportions and compositions are entirely consistent with those of magnesian suite rocks, see Figure 1 and Tables 1 - 3. Mafic silicate minerals in clast U have Mg# of 79-83; olivine is slightly more ferroan than pyroxenes, as expected from Fe-Mg equilibrium. Plagioclase compositions range from An97 to An90, as expected in a rock of the magnesian suite (Table 1, Fig. 1). The range of plagioclase compositions implies incomplete chemical equilibrium (consistent with the range of Ca contents in pigeonite, Fig. 4); plutonic rocks of the magnesian suite typically have plagioclase of limited compositional ranges (James and Flohr 1983). The average plagioclase composition in clast U is ~ An96; thus, if it had equilibrated completely, it would not be distinct in Figure 1 from the granulite and anorthosite clasts in ALHA81005.

James and Flohr (1983) divided rocks of the magnesian suite into two chemically distinct groups, magnesian norites and magnesian gabbronorites, based on the compositions of their major minerals and the presence or absence of certain minor minerals (Table 5). Magnesian suite norites and gabbronorites can be distinguished also by the minor element chemistry of their pyroxenes (Bersch et al. 1991; Norman et al. 1995), particularly their abundances of Ti and Cr. From published discriminants (James and Flohr 1983; Bersch et al. 1991; Norman et al. 1995), clast U is more closely related to the magnesian norites in having a higher Mg#, more low-Ca pyroxene than augite, and minor minerals rich in Ti (Table 5). In addition, the pyroxenes of clast U have Ti abundances and FeO/MgO ratios that fall in and near the field defined for magnesian norites (Fig. 8a); a slight enlargement of that field (Norman et al. 1995) would encompass the pyroxenes of clast U.

However, clast U does not share all the published characteristics of magnesian norites, beyond its lack of zircon and potassium feldspar (which could be ascribed to the clast's small size). The Cr abundances in the pyroxenes are consistent with magnesian gabbronorite and not norite (Fig. 8b). Similarly, the low Ni and Co contents of its olivine are more consistent with magnesian gabbronorites than with norites (Longhi et al. 2010; Fig. 9). So, clast U has similarities with both magnesian norites and gabbronorites, but is not fully consistent with either.

**Variety within the Magnesian Suite**

Although clast U is likely an impact melt, and thus could represent a mix of multiple protoliths, its mineralogical and mineral-chemical affinity with the magnesian suite is clear. However, its mineralogy and mineral chemistry are not an exact match to those of magnesian suite rocks in the Apollo magnesian collection, notably its norites and gabbronorites (Table 5). This disparity may suggest that the lunar magnesian suite could be more diverse than in the Apollo collection. A putative magnesian suite protolith for clast U could have contained more Ti than parent magmas of magnesian gabbronorites (despite having higher Mg# and thus being less fractionated; Fig. 8a), and could have contained less Cr than a magnesian norite (despite having comparable Mg#s; Fig. 8b. In other words, one could not derive a putative magnesian suite protolith for clast U by fractionation of magmas parental to Apollo magnesian norites or gabbronorites.

Even among the Apollo samples, the magnesian suite may be more diverse than generally appreciated. Lindstrom et al. (1989) presented evidence that the field of the magnesian suite on Figure 1 is not a differentiation trend, but by implication represents a series of distinct magmas within the (broadly construed) suite of magnesian plutonic rocks.

**Magnesian Suite Rocks Across the Whole Moon**

At this time, clast U (or to be exact its protolith) is the only documented fragment of rock related to the magnesian suite from a lunar sample inferred to have originated far from the

Apollo sites (Pieters et al. 1983; Kallemeyn and Warren 1983; Korotev et al. 1983; Isaacson et al. 2013). Many granulites from lunar highlands meteorites (many inferred to have come from the far side) have mineral compositions, An and Mg#, like those of the magnesian suite (Fig. 1; e.g., Cahill et al. 2004; Treiman et al. 2010; Gross et al. 2014). However, these granulites show no evidence of a KREEP signature as in rocks of the Apollo magnesian suite. Clast U is thus an 'exception that proves the rule' of the rarity of magnesian suite materials among lunar highlands meteorites. The apparent rarity of magnesian suite rocks in lunar meteorites does not reflect an inability to detect them – they truly are rare.

Although clast U sits in ALHA 81005, a regolith breccia inferred to be from the lunar farside, we have no evidence that clast U originated on the farside. Rather, it (as an impact melt rock) could have formed on the lunar nearside where magnesian suite material is relatively common (Jolliff et al. 2000; Elardo et al. 2011), and been transported to the lunar farside by meteoroid impacts. In fact, ALHA 81005 does contain a distinct contribution of non-local material, as shown by its clasts of several sorts of mare basalts (Robinson et al. 2012).

Per the Elardo et al. (2011) quote in the Introduction, the search for fragments of magnesian suite materials should continue. Recognition of magnesian suite materials (or their absence) has important implications for lunar geologic and thermal history. One should look for clasts with highly magnesian mafic minerals that have Fe/Mn consistent with a lunar origin (Karner et al. 2003; Gross et al. 2010). The presence of plagioclase more sodic than ~An95 would distinguish such clasts from magnesian anorthosites, feldspathic granulites, and impact melts from them. Minor minerals (or mineral compositions) indicative of a KREEP contribution would help tie such rock fragments to the magnesian suite as known in the Apollo collection, but might not be seen in hypothetical KREEP-poor magnesian suite rocks. Non-chondritic metal compositions would argue against an impact-melt origin (but see Papike et al. 1991). A complication in this search for rock fragments of the magnesian suite is the presence of meteorite fragments, documented in both Apollo samples and lunar highlands meteorites (Rubin 1997; Zolensky 1997; Day et al. 2006; Joy et al. 2012). These meteorite fragments can contain highly magnesian olivine and plagioclase with moderate Na content, but would likely not have a high Fe/Mn like lunar materials, and could have textures consistent with primitive meteorites (e.g., Day et al. 2006; Joy et al. 2012 – individual mineral grains derived from meteoritic infall could be difficult to distinguish from indigenous lunar materials.

## IMPLICATIONS

Clast U is now the only documented fragment of rock related to the lunar magnesian suite from a source outside the Apollo landing sites. Clast U is not a fragment of magnesian suite rock *per se*, of which all known examples are plutonic; rather, the mineralogy and mineral chemistry of Clast U are similar to those of some magnesian suite rocks (norite & gabbronorite). The mineralogy and mineral chemistry of Clast U are not exact matches to any known rock of the magnesian suite, so the magnesian suite may be more diverse than currently understood. It is possible that Clast U formed originally on the lunar nearside and was transported by impact into the lunar farside regolith sampled by ALHA81005 (Isaacson et al. 2013). In any case, Clast U demonstrates that rock related to the lunar magnesian suite can be recognized in lunar highlands meteorites, and that the rarity of magnesian suite materials in highlands meteorites is real. This rarity suggests that magnesian suite materials are not widespread on the Moon, but may be localized around the Apollo sampling sites (e.g., near the Procellarum KREEP terrane).

## ACKNOWLEDGMENTS

We are grateful to: D.K. Ross and A. Peslier (JSC) for assistance with electron microprobe analyses; to the A.E.; and to M.D. Norman, R. Korotev, and Y. Liu for extremely helpful reviews. This work was supported in part by NASA Cosmochemistry Grant NNX12AH64G to AHT, and a subcontract to JG from the NASA Lunar Science Institute node at the LPI (contract NNA09DB33A: D.A. Kring, PI). Lunar and Planetary Institute Contribution #1xxx.

## REFERENCES

Arai, T., Otsuki, M., Ishii, T., Mikouchi, T., and Miyamoto, M. (2005) Mineralogy of Yamato 983885 lunar polymict breccia with a KREEP basalt, a high-Al basalt, a very low-Ti basalt and Mg-rich rocks. *Antarctic Meteorite Research*, 18, 17-45.

Bersch, M.G., Taylor, G.J., Keil, K., and Norman, M.D. (1991) Mineral compositions in pristine lunar highlands rocks and the diversity of highlands magmatism. *Geophysical Research Letters*, 18, 2085-2088.

Biehl, L., and Landgrebe, D. (2002) MultiSpec – A tool for multispectral-hyperspectral image data analysis. *Computers and Geosciences*, 28, 1153–1159.

Boynton, W.V, and Hill, D.H. (1983) Composition of bulk samples and a possible pristine clast from Allan Hills A81005. *Geophysical Research Letters*, 10, 837-840.

Cahill, J.T., Floss, C., Anand, M., Taylor, L.A., Nazarov, M.A., and Cohen, B.A. (2004) Petrogenesis of lunar highlands meteorites: Dhofar 025, Dhofar 081, Dar al Gani 262, and Dar al Gani 400. *Meteoritics and Planetary Science*, 39, 503-529.

Chakraborty, S. (2010) Diffusion coefficients in olivine, wadsleyite and ringwoodite. *Reviews in Mineralogy and Geochemistry*, 72, 603-639.

Daubar, I.J., Kring, D.A., Swindle, T.D., and Jull, A.J.T. (2002) Northwest Africa 482: A crystalline impact-melt breccia from the lunar highlands. *Meteoritics & Planetary Science*, 37, 1797-1813.

Day, J.M.D., Floss, C., Taylor, L.A., Anand, M., and Patchen, A.D. (2006) Evolved mare basalt magmatism, high Mg/Fe feldspathic crust, chondritic impactors, and the petrogenesis of

Antarctic lunar breccia meteorites Meteorite Hills 01210 and Pecora Escarpment 02007 *Geochimica et Cosmochimica Acta*, 70, 5957-5989.

Demidova, S.I., Nazarov, M.A., Taylor, L.A., and Patchen, A. (2003) Dhofar 304, 305, 306 and 307: New lunar highland meteorites from Oman. *Lunar and Planetary Science* 34th, Abstract #1285.

Elardo, S.M., Draper, D.S., and Shearer, C.K.Jr. (2011) Lunar Magma Ocean crystallization revisited: Bulk composition, early cumulate mineralogy, and the source regions of the highlands Mg-suite. *Geochimica et Cosmochimica Acta*, 75, 3024–3045

Elkins-Tanton, L.T., Burgess, S., and Yin, Q.-Y. (2011) The lunar magma ocean: Reconciling the solidification process with lunar petrology and geochronology. *Earth and Planetary Science Letter,s* 304, 326-336.

Fagan, A.L., Neal, C.R., Simonetti, A., Donohue, P.H., and O'Sullivan, K.M. (2013) Distinguishing between Apollo 14 impact melt and pristine mare basalt samples by geochemical and textural analyses of olivine. *Geochimica et Cosmochimica Acta*, 106, 429-445.

Gillis, J.J., Jolliff, B.L., and Korotev, R.L. (2004) Lunar surface geochemistry: Global concentrations of Th, K, and FeO as derived from lunar prospector and Clementine data, *Geochimica et Cosmochimica Acta*, 68, 3791-3805.

Goldoff, B., Webster, J.D., and Harlov, D.E. (2012) Characterization of fluor-chlorapatites by electron probe microanalysis with a focus on time-dependent intensity variation of halogens. *American Mineralogist*, 97, 1103-1115.

Goodrich, C.A., Taylor, G.J., Keil, K., Boynton, W.V., and Hill, D.H. (1984) Petrology and chemistry of hyperferroan anorthosites and other clasts from lunar meteorite ALHA81005. *Proceedings Lunar Planetary Science Conference 15th*, in *Journal of Geophysical Research*, 89, C87-C94.

Goodrich, C.A., Taylor, G.J., and Keil K. (1985) An apatite-rich, ferroan, mafic lithology from lunar meteorite ALHA81005. *Proceedings Lunar Planetary Science Conference 16th*, in *Journal of Geophysical Research*, 90, C405-C414.

Gross, J., and Treiman, A. H. (2010) Dispersed Fe/Mn ratios of lunar rocks: ALHA 81005's view from the farside. *Goldschmidt Conference 2010,* Abstract #2557.

 

Gross, J., and Treiman, A.H. (2011) Unique spinel-rich lithology in lunar meteorite ALHAA81005: Origin and possible connection to $M^3$ observations of the farside highlands. *Journal of Geophysical Research*, 116, E10009.

Gross, J., Treiman, A.H., and Mercer, C.N. (2014) Lunar feldspathic meteorites: Constraints on the geology of the lunar highlands, and the origin of the lunar crust. *Earth and Planetary Science Letters*, 388, 318-328.

Haggerty, S.E. (1973) Armalcolite and genetically associated opaque minerals in the lunar samples. *Proceedings of the Fourth Lunar Science Conference* (Supplement 4 to *Geochimica et Cosmichimica Acta*), vol. 1, 777-797.

Isaacson, P.J., Hiroi, T., Hawke, B.R., Lucey, P.G., Pieters, C.M., Liu, Y., Patchen, A., and Taylor, L.A. (2013) Lunar meteorite geologic context: New constraints from VNIR spectroscopy and geochemistry. *Lunar and Planetary Science Conference* 44$^{th}$, Abstract #1134.

James, O.B., and Flohr, M.K. (1983) Subdivision of the Mg-suite noritic rocks into Mg-gabbronorites and Mg-norites. *Proceedings Thirteenth Lunar and Planetary Science Conference Part 2, Journal of Geophysical Research*, 88, A603-A614.

Jolliff, B.L., Korotev, R.L., and Haskin, L.A. (1991) A ferroan region of the lunar highlands as recorded in meteorites MAC 88104 and MAC 88105. *Geochimica et Cosmochimica Acta*, 55, 3051–3071.

Jolliff, B.L., Gillis, J.J., Haskin, L.A., Korotev, R.L., and Wieczorek, M.A. (2000) Major lunar crustal terranes: surface expressions and crust-mantle origins. *Journal of Geophysical Research*, 105, 4197–4416.

Joy, K.H., Zolensky, M.E., Nagashima, K., Huss, G.R., Ross, D.K., McKay, D.S., and Kring, D.A. (2012) Direct detection of projectile relics from the end of the lunar basin–forming epoch. *Science*, 336, 1426-1429.

Kallemeyn, G.W., and Warren, P.H. (1983) Compositional implications regarding the lunar origin of the ALHA81005 meteorite. *Geophysical Research Letters*, 10, 833-836.

Karner, J., Papike, J.J. and Shearer, C.K. (2003) Olivine from planetary basalts: Chemical signatures that indicate planetary parentage and those that record igneous setting and process. *American Mineralogist*, 88, 806-816.

Kobayashi, S., Karouji, Y., Morota, T., Takeda, H., Hasebe, N., Hareyama, M., Kobayashi, M., Shibamura, E., Yamashita, N., d'Uston, C., Gasnault, O., Forni, O., Reedy, R.C., Kim, K.J., and Ishihara, Y. (2012) Lunar farside Th distribution measured by Kaguya gamma-ray spectrometer. *Earth and Planetary Science Letters*, 337-338, 10-16.

Korotev, R.L. (2005) Lunar geochemistry as told by lunar meteorites. *Chemie der Erde*, 65, 297-346.

Korotev, R.L. The Lunar Meteorite List (2014) http://meteorites.wustl.edu/lunar/moon_meteorites_list_alumina.htm#DHO303. Viewed April 2014.

Korotev, R.L., and Jolliff, B.L. (2001) The curious case of the lunar magnesian granulitic breccias. *Lunar and Planetary Science Conference,* 32nd, Abstract #1455.

Korotev, R.L., Lindstrom, M.M., Lindstrom, D.J., and Haskin, L.A. (1983) Antarctic meteorite ALHA81005—Not just another lunar anorthositic norite. *Geophysical Research Letters*, 10, 829–832.

Korotev, R.L., Jolliff, B.L., Zeigler, R.A., Gillis, J.J., and Haskin, L.A. (2003) Feldspathic lunar meteorites and their implications for compositional remote sensing of the lunar surface and the composition of the lunar crust. *Geochimica et Cosmochimica Acta*, 67, 4895–4923.

Korotev, R.L., Zeigler, R.A., and Jolliff, B.L. (2006) Feldspathic lunar meteorites Pecora Escarpment 02007 and Dhofar 489: Contamination of the surface of the lunar highlands by post-basin impacts. *Geochimica et Cosmochimica Acta,* 70, 5935-5957.

Korotev, R.L., Zeigler, R.A., Jolliff, B.L., Irving, A.J., and Bunch, T.E. (2009) Compositional and lithological diversity among brecciated lunar meteorites of intermediate iron composition. *Meteoritics and Planetary Science*, 44, 1287–1322.

Korotev, R.L., Jolliff, B.L., and Zeigler, R.A. (2012) What lunar meteorites tell us about the lunar highlands crust. *Second Conference on the Lunar Highland Crust*. Abstract # 9003.

Kurat, G., and Brandstätter, F. (1983) Meteorite ALHA81005: Petrology of a new lunar highland sample. *Geophysical Research Letters*, 10, 795-798

Lindstrom, M.M., Marvin, U.B., and Mittlefehldt, D.W. (1989) Apollo 15 Mg- and Fe-norites: A redefinition of the Mg-suite differentiation trend. *Proceedings of the 19th Lunar and Planetary Science Conference*, pp. 245-254.

Liu, Y., Patchen, A., and Taylor, L.A. (2011) Lunar highland breccias MIL 090034/36/70/75: A significant KREEP component. *Lunar and Planetary Science* 42nd, Abstract #1261.

Longhi, J., Durand, S.R., and Walker, D. (2010) The pattern of Ni and Co abundances in lunar olivines. *Geochimica et Cosmochimica Acta,* 74, 784-798.

Lydon, J.W. (2005) *The Measurement of the Modal Mineralogy of Rocks from SEM Imagery: The Use of Multispec© and ImageJ Freeware*. Geological Survey of Canada, Open File 4941, 37p.

Maloy A.K., and Treiman, A.H. (2007) Evaluation of image classification routines for determining modal mineralogy of rocks from X-ray maps *American Mineralogist*, 92, 1781–1788.

Marvin, U.B. (1983) The discovery and initial characterization of Allan Hills 81005: The first lunar meteorite. *Geophysical Research Letters*, 10, 775-778.

Marvin, U.B., and Holmberg, B. (1992) Highland and mare components in the Calcalong Crek lunar meteorite. *Lunar and Planetary Science* XXIII, 849-850.

McCallum, I.S. (1996) The Stillwater Complex, p. 441–483 *in* Cawthorn, R.G., ed., *Layered Intrusions.* Amsterdam, Elsevier Science.

McCallum, I.S., and Schwarz, J.M. (2001) Lunar Mg suite: Thermobarometry and petrogenesis of parental magmas. *Journal of Geophysical Research*, 106, 27,969-27,983.

Norman, M.D., and Ryder, G. (1980) Geochemical constraints on the igneous evolution of the lunar crust. *Proceedings 11th Lunar and Planetary Science Conference,* 317-331.

Norman, M.D., Keil, K., Griffin, W.L., and Ryan, G.C. (1995) Fragments of ancient lunar crust: Petrology and geochemistry of ferroan noritic anorthosites from the Descartes region of the Moon. *Geochimica et Cosmochimica Acta,* 59, 831-847.

Ostertag, R. (1983) Shock experiments on feldspar crystals. *Proceedings 14th Lunar and Planetary Science Conference Part 1, Journal of Geophysical Research*, 88, B364-B376.

Papike, J.J., Taylor, L, and Simon, S. (1991) Lunar Minerals. Ch. 5 in Heiken G.H., Vaniman D.T, and French B.M., eds. *The Lunar Sourcebook: A user's guide to the Moon*. CUP Archive.

Papike, J.J., Fowler, G.W., Adcock, C.T, and Shearer, C.K. (1999) Systematics of Ni and Co in olivine from planetary melt systems: Lunar mare basalts. *American Mineralogist*, 84, 392–399.

Petry, C., Chakraborty, S., and Palme, H. (2004) Experimental determination of Ni diffusion coefficients in olivine and their dependence on temperature, composition, oxygen fugacity, and crystallographic orientation. *Geochimica et Cosmochimica Acta,* 68, 4179-4188.

Pieters, C.M., Hawke, B.R., Gaffey, M., and McFadden, L.A. (1983) Possible source areas of meteorite ALHA81005: Geochemical remote sensing information. *Geophysical Research Letters*, 10, 813-816.

Qian, Q., O'Neill H.St.C., and Hermann, J. (2010) Comparative diffusion coefficients of major and trace elements in olivine at ~950 °C from a xenocryst included in dioritic magma. *Geology*, 38, 331-334.

Raedeke, L.D., and McCallum, I. S. (1980) A comparison of fractionation trends in the lunar crust and the Stillwater Complex. 133-153 *in* Papike, J.J. and MerrilL R.B., eds. *Proceedings of the Conference on the Highlands Lunar Crust*. Lunar and Planetary Institute, Houston.

Robinson, K.L., Treiman, A.H., and Joy, K.H. (2012) Basaltic fragments in lunar highlands meteorites: Connecting sample analyses to orbital remote sensing. *Meteoritics and Planetary Sciences*, 47, 387-399.

Rubin, A.E. (1997) The Hadley Rille enstatite chondrite and its agglutinate-lile rim: Impact melting during accretion to the Moon. *Meteoritics and Planetary Sciences* 32, 135-141.

Ryder, G. and Ostertag, R. (1983) ALHA 81005: Moon, Mars, petrography, and Giordano Bruno. *Geophysical Research Letters* 10, 791-794.

Ryder, G., Norman, M.D., and Score, R.A. (1980) The distinction of pristine from meteorite-contaminated highlands rocks using metal compositions. *Proceedings Lunar Planetary Science Conference 11th*, 471-479.

Shearer, C.K. and Papike, J.J. (1999) Magmatic evolution of the Moon. *American Mineralogist*, 84, 1469-1494.

Shearer, C.K., and Papike, J.J. (2005) Early crustal building processes on the Moon: Models for the petrogenesis of the magnesian suite. *Geochimica et Cosmochimica Acta*, 69, 3445–3461.

Shearer, C.K., Hess, P.C., Wieczorek, M.A., Pritchard, M.E., Parmentier, E.M., Borg, L.E., Longhi, J., Elkins-Tanton, L.T., Neal, C.R., Antonenko, I., Canup, R.M., Halliday, A.N., Grove, T.L., Hager, B.H., Lee, D.-C., and Wiechert, U. (2006) Thermal and magmatic evolution of the Moon. *Reviews of Mineralogy and Geochemistry*, 60, 365-518.

Smith, J.V., and Steele, I.M. (1976) Lunar mineralogy; a heavenly detective story; Part II. *American Mineralogist*, 61, 1059-1116.

Sokol, A.K., Fernandes, V.A., Schulz, T., Bischoff, A., Burgess, R., Clayton, R.N., Münker, C., Nishiizumi, K., Palme, H., Schultz, L., Weckwerth, G., Mezger, K., and Horstmann, M. (2008) Geochemistry, petrology and ages of the lunar meteorites Kalahari 008 and 009: New constraints on early lunar evolution. *Geochimica et Cosmochimica Acta*, 72, 4845–4873.

Snape, J.E., Joy, K.H., and Crawford, I.A. (2011) Characterization of multiple lithologies within the lunar feldspathic regolith breccia meteorite Northeast Africa 001. *Meteoritics and Planetary Science*, 46, 1288–1312.

Snyder, G.A., Neal, C.R., Taylor, L.A., and Halliday, A.N. (1995) Processes involved in the formation of magnesian-suite plutonic rocks from the highlands of the Earth's Moon *Journal of Geophysical Research*, 100, 9365-9388.

Stanin, F.T., and Taylor, L.A. (1980) Armalcolite: An oxygen fugacity indicator. *Proceedings Lunar and Planetary Science Conference* 11th, 117-124.

Stöffler, D., Bischoff, A., Borchardt, R., Burghele, A., Deutsch, A., Jessberger, E. K., Ostertag, R., Palme, H., Spettel, B., Reimold, W.U., Wacker, K. and Wänke H., (1985) Composition and evolution of the lunar crust in the Descartes highlands, Apollo 16. *Proceedings Lunar and Planetary Science Conference 15th, Journal of Geophysical Research* 90, C449–C506.

Takeda, H., Yamaguchi, A., Bogard, D.D., Karouji, Y., Ebihara, M., Ohtake, M., Saiki, K., and Arai, T. (2006) Magnesian anorthosites and a deep crustal rock from the farside crust of the Moon. *Earth and Planetary Science Letters*, 247, 171–184.

Taylor, G.J., Warren, P., Ryder, G., Delano, J., Pieters, C., and Lofgren, G. (1991) Lunar Rocks, p. 183-284 (Ch. 6) *in* Heiken, G., Vaniman, D., and French, B. (eds) *Lunar Sourcebook*. Cambridge University Press, N.Y.

Treiman, A.H., and Drake, M.J. (1983) Origin of lunar meteorite ALHA81005: Clues from the presence of terrae clasts and a very low-titanium mare basalt clasts. *Geophysical Research Letters*, 10, 783-786.

This is a preprint, the final version is subject to change, of the American Mineralogist (MSA)
Cite as Authors (Year) Title. American Mineralogist, in press.
(DOI will not work until issue is live.) DOI: http://dx.doi.org/10.2138/am-2015-4800 

Treiman, A.H., and Gross, J. (2013) Basalt related to lunar Mg-suite plutonic rocks: A fragment in lunar meteorite ALHA81005. *73rd Annual Conference, Meteoritical Society*, Abstract #5183.

Treiman, A.H., Maloy, A.K., Shearer, C.K.Jr., and Gross, J. (2010) Magnesian anorthositic granulites in lunar meteorites in lunar meteorites Allan Hills 81005 and Dhofar 309: Geochemistry and global significance. *Meteoritics and Planetary Science*, 45, 163-180.

Vaniman, D.T., and Papike, J.J. (1980) Lunar highland melt rocks: Chemistry, petrology and silicate mineralogy. P. 271-337 in *Proceedings of the Conference on the Lunar Highlands Crust* (R.B. Merrill and J.J. Papike, eds). Pergamon.N.Y.

Warren, P.H. (2012) Let's get real: Not every lunar rock sample is big enough to be representative for every purpose (abstract). *Second Conference on the Lunar Highlands Crust,* 59-60. *LPI Contribution #1677*.

Warren, P.H., Taylor, G.J., and Keil, K. (1983) Regolith breccia Allan Hills A81005: Evidence of lunar origin, and petrography of pristine and nonpristine clasts. *Geophysical Research Letters*, 10, 779-782.

Wieczorek M.A., Jolliff B.L., Khan A., Pritchard M.E., Weiss B.P., Williams J.G., Hood L.L., Righter K., Neal C.R., Shearer C.K., McCallum I.S., Tompkins S., Hawke B.R., Peterson C., Gillis J.J., and Bussey B. (2006) The Constitution and Structure of the Lunar Interior. pp. 221-364 in *Reviews in Mineralogy & Geochemistry*, 60, Mineralogical Society of America

Williams, H., Turner, F.J., and Gilbert, C.M. (1954) *Petrography: An Introduction to the Study of Rocks in Thin Sections*. W.H. Freeman, San Francisco. 406 p.

Wittmann, A., and Korotev, R.L. (2013) Iron-nickel (-cobalt) metal in lunar rocks revisited (abstract). *Lunar and Planetary Science Conference* 44th, Abstract #3035.

Wood, J.A., Dickey, J.S.Jr., Marvin, U.B., and Powell, B.J. (1970) Lunar anorthosites and a geophysical model of the Moon. *Proceedings of the Apollo 11 Lunar Science Conference 1*, 965-988.

Yamaguchi, A., Karouji, Y., Takeda, H., Nyquist, L., Bogard, D., Ebihara, M., Shih, C.-Y., Reese, Y., Garrison, D., Park, J., and McKay, G. (2010) The variety of lithologies in the Yamato-86032 lunar meteorite: Implications for formation processes of the lunar crust. *Geochimica et Cosmochimica Acta*, 74, 4507–4530.

Zolensky, M.E. (1997) Structural water in the Bench Crater chondrite returned from the Moon. *Meteoritics and Planetary Science*, 32, 15-18.

The authors declare that they have no competing commercial interests, or other interests that might be perceived to influence the results and/or discussion reported in this paper.

Correspondence and requests for materials should be addressed to A.H. Treiman.

Figure 1. Mg# of mafic minerals, molar Mg/(Mg+Fe), versus An content of plagioclase, molar Ca/(Ca+Na), for selected lunar samples. Fields of 'Ferroan Anorthosite' and 'Magnesian Suite' are defined by Apollo returned samples (Warren et al 1983b; Shearer and Papike 2005). Other materials are: black rectangle, clast U of ALHA81005, this work; star, clast 25.8 of Dhofar 025 (Cahill et al. 2004); black circle, selected clasts in Dhofar 305 and 307 (Demidova et al. 2003); and gray rectangle, 'An93 anorthosite' of Y86032 (Yamaguchi et al. 2010.). Light-gray ellipse approximates field of magnesian granulites and anorthosites of most lunar highlands meteorites, and darker gray ellipse approximates field of granulites and anorthosites of ALHA81005 (Gross et al., 2014).

Figure 2. Transmitted light images. [a] Mosaic of thin section ALHA81005,9; fragments of anorthosites and granulites in a glassy agglutinitic matrix. Clast U denoted by arrow. [b] Clast U, with typical impactite to upper right. See Fig. 2 for mineral identifications – olivine and pyroxene are colorless here, indicative of their high Mg#s.

Figure 3. Back-scattered electron (BSE) images. [a] Clast U,'plag' is plagioclase, 'ol' is olivine, 'pig' is pigeonite, 'aug' is augite, 'sil' is silica, 'tr' is troilite, and Fe is metal. Squares show locations of detail images. [b] Detail at right side of clast, showing extensively cracked plagioclase and uncracked plagioclase (probably amorphized or melted by shock). Note matrix glass to upper right of frame, with mineral fragments and round dark bubbles. [c] Detail of core of pyroxene in center of clast, showing intense cracking and lighter-tone blebby grains of augite in low-Ca pyroxene, probably exsolutions.

Figure 4. X-ray element maps of Clast U, showing distribution of major and minor minerals. [a] Red=Mg, Green=Ca, Blue=Al. 'plag'=plagioclase, 'ol'=olivine, 'pig'=pigeonite (low-Ca and high-Ca pigeonite noted), 'aug'=augite, bright green spots are apatite. Purple spot at lower left is a spinel grain in the matrix outside clast U. [b] Red=Ti, Green=Fe, Blue=Al. Rutile is bright red; ilmenite and armalcolite are yellow and orange.

Figure 5. Compositions of pyroxenes and olivine in the Ca-Mg-Fe quadrilateral. For pyroxene compositions (circles): Di = $CaMgSi_2O_6$, En = $CaFeSi_2O_6$, Fs = $Fe_2Si_2O_6$, En = $Mg_2Si_2O_6$. Olivine compositions (triangles) plotted as Mg-Fe. Dashed field encloses all compositions of mare basalt pyroxenes (Papike et al. 1991).

Figure 6. Minor elements in pyroxenes of clast U.

Figure 7. EDS spectrum of an apatite grain in Clast U (see Fig. B). Strong peaks for F_Kα and ClKα X-rays show that the grain is apatite, and not merrillite. Peaks for Si and Fe are from surrounding minerals. The apatite grains are too small for quantitative analyses.

Figure 8. Pyroxene compositions in clast U compared to those of lunar highlands lithologies, after Bersch et al. (1991) and Norman et al. (1995). (a) Low-Ca pyroxene compositions are

 

consistent with clast U being related to Mg-norites. (b) High-Ca pyroxene compositions, in contrast, are more similar to those of Mg-gabbronorites.

Figure 9. Nickel and cobalt in Clast U olivine (filled square) compared to those of olivine in other lunar lithologies (Longhi et al. 2010), including magnesian feldspathic granulites. Uncertainties on Ni and Co are 2 standard error of mean for 17 individual analyses, see Table 3. Dashed lines are 3σ detection limits for Ni and Co, based on sum of all individual analyses. Data from Papike et al. (1999), Shearer and Papike (2005), and Treiman et al. (2010).

Table 1. Plagioclase and Olivine Compositions: Clast U.

| | plagioclase 3/5 | plagioclase 1/1 | plagioclase 3/1 | plagioclase 1206 9/17 | olivine L8 9/2 | olivine L4 5/5 | olivine L6 7/3 | olivine L7 8/3 |
|---|---|---|---|---|---|---|---|---|
| $SiO_2$ | 43.65 | 43.63 | 43.50 | 43.21 | 39.22 | 39.53 | 39.34 | 38.88 |
| $TiO_2$ | 0.01 | 0.02 | 0.02 | 0.00 | 0.05 | 0.03 | 0.08 | 0.08 |
| $Al_2O_3$ | 35.79 | 35.85 | 35.63 | 34.32 | 0.01 | 0.02 | 0.00 | 0.02 |
| $Cr_2O_3$ | - | - | - | 0.00 | 0.05 | 0.04 | 0.03 | 0.05 |
| FeO | 0.09 | 0.21 | 0.11 | 0.23 | 20.02 | 16.63 | 19.26 | 19.92 |
| NiO | - | - | - | - | 0.01 | 0.00 | 0.00 | 0.03 |
| CoO | - | - | - | - | 0.00 | 0.00 | 0.00 | 0.01 |
| MnO | 0.01 | 0.00 | 0.00 | 0.02 | 0.27 | 0.22 | 0.29 | 0.29 |
| MgO | 0.12 | 0.10 | 0.12 | 0.17 | 40.70 | 43.58 | 41.38 | 41.14 |
| CaO | 19.69 | 19.18 | 19.58 | 18.9 | 0.09 | 0.09 | 0.11 | 0.08 |
| $Na_2O$ | 0.28 | 0.37 | 0.4 | 1.16 | 0.00 | 0.00 | 0.01 | 0.00 |
| $K_2O$ | 0.01 | 0.02 | 0.01 | 0.09 | 0.00 | 0.00 | 0.01 | 0.00 |
| $P_2O_5$ | - | - | - | - | 0.02 | 0.01 | 0.00 | 0.01 |
| $ZrO_2$ | - | - | - | 0.00 | 0.02 | 0.01 | 0.02 | 0.00 |
| Total | 99.67 | 99.38 | 99.28 | 98.10 | 100.47 | 100.16 | 100.52 | 100.49 |
| | | | | | | | | |
| Normalization To Cations | 5 | 5 | 5 | 5 | 3 | 3 | 3 | 3 |
| Si | 2.025 | 2.029 | 2.028 | 2.024 | 1.005 | 0.998 | 1.003 | 0.994 |
| Ti | 0.000 | 0.001 | 0.000 | 0.000 | 0.001 | 0.001 | 0.002 | 0.001 |
| Al | 1.957 | 1.965 | 1.956 | 1.895 | 0.000 | 0.001 | 0.000 | 0.001 |
| Cr | - | - | - | 0.000 | 0.001 | 0.001 | 0.001 | 0.001 |
| Fe | 0.004 | 0.008 | 0.004 | 0.009 | 0.429 | 0.351 | 0.411 | 0.426 |
| Ni | - | - | - | - | 0.000 | 0.000 | 0.000 | 0.001 |
| Co | - | - | - | - | 0.000 | 0.000 | 0.000 | 0.000 |
| Mn | 0.001 | 0.000 | 0.000 | 0.001 | 0.006 | 0.005 | 0.006 | 0.006 |
| Mg | 0.008 | 0.007 | 0.008 | 0.012 | 1.554 | 1.641 | 1.573 | 1.568 |
| Ca | 0.979 | 0.956 | 0.977 | 0.949 | 0.003 | 0.002 | 0.003 | 0.002 |
| Na | 0.025 | 0.034 | 0.028 | 0.105 | 0.000 | 0.000 | 0.001 | 0.000 |
| K | 0.000 | 0.001 | 0.001 | 0.002 | 0.000 | 0.000 | 0.000 | 0.000 |
| P | - | - | - | - | 0.000 | 0.000 | 0.000 | 0.000 |
| Zr | - | - | 0.000 | 0.000 | 0.000 | 0.000 | 0.000 | 0.000 |
| *Charge* | *-0.020* | *0.015* | *-0.013* | *-0.170* | *0.011* | *0.000* | *0.010* | *-0.008* |
| | | | | | | | | |
| Fo | | | | | 78.6 | 82.4 | 79.3 | 78.7 |
| CaOl | | | | | 0.1 | 0.1 | 0.2 | 0.1 |
| An | 97.5 | 96.4 | 97.2 | 89.6 | | | | |
| Ab | 2.5 | 3.4 | 2.7 | 9.9 | | | | |
| Or | 0.0 | 0.1 | 0.01 | 0.5 | | | | |

As analyzed here. Molar proportions are: Olivine, Fo - $Mg_2SiO_4$, CaOl - $Ca_2SiO_4$; plagioclase An – anorthite, Ab – albite, Or - orthoclase. *Charge* is total charge on mineral formula, ideally is zero.

.

Table 2. Pyroxene Compositions: Clast U.

| | pigeonite L1 2/26 | pigeonite L1 2/16 | pigeonite L1 6/15 | pigeonite L2 3/11 | augite L3 4/05 | augite L5 6/08 | augite L2 3/28 | augite L3 4/13 |
|---|---|---|---|---|---|---|---|---|
| $SiO_2$ | 55.55 | 55.52 | 55.14 | 55.10 | 54.20 | 55.31 | 51.24 | 51.16 |
| $TiO_2$ | 0.22 | 0.18 | 0.21 | 0.26 | 0.98 | 0.25 | 2.17 | 2.70 |
| $Al_2O_3$ | 1.32 | 1.23 | 1.46 | 1.34 | 1.22 | 1.15 | 2.41 | 2.25 |
| $Cr_2O_3$ | 0.56 | 0.52 | 0.59 | 0.54 | 0.37 | 0.52 | 0.47 | 0.45 |
| FeO | 10.76 | 10.73 | 10.11 | 10.12 | 12.51 | 7.71 | 9.11 | 7.65 |
| NiO | 0.00 | 0.01 | 0.00 | 0.01 | 0.00 | 0.03 | 0.01 | 0.00 |
| CoO | 0.01 | 0.02 | 0.00 | 0.00 | 0.00 | 0.00 | 0.00 | 0.00 |
| MnO | 0.25 | 0.26 | 0.25 | 0.28 | 0.33 | 0.23 | 0.25 | 0.24 |
| MgO | 29.02 | 28.95 | 27.97 | 26.68 | 22.50 | 24.68 | 17.17 | 16.83 |
| CaO | 2.21 | 2.84 | 4.15 | 6.20 | 8.55 | 10.64 | 17.62 | 19.10 |
| $Na_2O$ | 0.01 | 0.00 | 0.02 | 0.01 | 0.01 | 0.01 | 0.09 | 0.13 |
| $K_2O$ | 0.00 | 0.00 | 0.00 | 0.00 | 0.00 | 0.01 | 0.00 | 0.00 |
| $P_2O_5$ | 0.03 | 0.00 | 0.01 | 0.01 | 0.00 | 0.00 | 0.02 | 0.03 |
| $ZrO_2$ | 0.00 | 0.00 | 0.00 | 0.00 | 0.00 | 0.00 | 0.00 | 0.00 |
| Total | 99.95 | 100.26 | 99.92 | 100.54 | 100.67 | 100.56 | 100.57 | 100.54 |
| Normalization To 4 Cations | | | | | | | | |
| Si | 1.973 | 1.967 | 1.963 | 1.960 | 1.969 | 1.972 | 1.888 | 1.884 |
| Ti | 0.006 | 0.005 | 0.006 | 0.007 | 0.027 | 0.007 | 0.060 | 0.075 |
| Al | 0.055 | 0.051 | 0.061 | 0.056 | 0.052 | 0.048 | 0.104 | 0.098 |
| Cr | 0.016 | 0.015 | 0.016 | 0.015 | 0.011 | 0.015 | 0.014 | 0.013 |
| Fe | 0.320 | 0.318 | 0.301 | 0.301 | 0.380 | 0.230 | 0.281 | 0.236 |
| Ni | 0.000 | 0.000 | 0.000 | 0.000 | 0.000 | 0.001 | 0.000 | 0.000 |
| Co | 0.000 | 0.000 | 0.000 | 0.000 | 0.000 | 0.000 | 0.000 | 0.000 |
| Mn | 0.008 | 0.008 | 0.008 | 0.008 | 0.010 | 0.007 | 0.008 | 0.008 |
| Mg | 1.537 | 1.529 | 1.484 | 1.415 | 1.218 | 1.312 | 0.943 | 0.924 |
| Ca | 0.084 | 0.108 | 0.158 | 0.237 | 0.333 | 0.407 | 0.695 | 0.754 |
| Na | 0.001 | 0.000 | 0.001 | 0.001 | 0.001 | 0.001 | 0.007 | 0.009 |
| K | 0.000 | 0.000 | 0.000 | 0.000 | 0.000 | 0.000 | 0.000 | 0.000 |
| P | 0.001 | 0.000 | 0.000 | 0.000 | 0.000 | 0.000 | 0.001 | 0.001 |
| Zr | 0.000 | 0.000 | 0.000 | 0.000 | 0.000 | 0.000 | 0.000 | 0.000 |
| *Charge* | *0.032* | *0.027* | *0.010* | *0.004* | *-0.043* | *0.019* | *0.012* | *0.027* |
| Wo | 4.3 | 5.5 | 8.1 | 12.1 | 17.2 | 20.9 | 36.2 | 39.4 |
| En | 79.2 | 78.2 | 76.4 | 72.5 | 63.1 | 67.3 | 49.1 | 48.3 |
| Fs | 16.5 | 16.3 | 15.5 | 15.4 | 19.7 | 11.8 | 14.6 | 12.3 |

As analyzed here. Molar proportions are: Wo = $CaSiO_3$; En = $MgSiO_3$; Fs = $MgSiO_3$. *Charge* is total charge on mineral formula, ideally is zero.

Table 4. Oxide Minerals in Clast U.

| | armalcolite | *armalcolite | ilmenite | ilmenite | chromite |
|---|---|---|---|---|---|
| $SiO_2$ | 0.15 | 0.81 | 0.23 | 1.18 | 0.70 |
| $TiO_2$ | 69.81 | 66.87 | 52.59 | 51.76 | 2.34 |
| $Al_2O_3$ | 1.32 | 1.38 | 0.07 | 0.09 | 12.59 |
| $Cr_2O_3$ | 6.07 | 5.73 | 0.40 | 0.44 | 48.32 |
| FeO | 11.31 | 15.70 | 40.17 | 37.22 | 29.49 |
| NiO | 0.01 | - | 0.00 | 0.01 | 0.00 |
| CoO | 0.02 | - | 0.00 | 0.01 | 0.02 |
| MnO | 0.20 | 0.14 | 0.69 | 0.50 | 0.40 |
| MgO | 1.84 | 1.87 | 3.81 | 6.52 | 4.28 |
| CaO | 3.97 | 3.65 | 0.70 | 0.54 | 0.23 |
| $Na_2O$ | 0.00 | - | 0.00 | 0.01 | 0.05 |
| $K_2O$ | 0.01 | - | 0.00 | 0.01 | 0.00 |
| $P_2O_5$ | 0.00 | - | 0.00 | 0.00 | 0.01 |
| $ZrO_2$ | 3.93 | 3.66 | 0.02 | 0.00 | 0.01 |
| Total | 98.64 | 99.81 | 98.70 | 98.28 | 98.43 |
| Normalization To Cations | 3 | 3 | 2 | 2 | 3 |
| Si | 0.006 | 0.031 | 0.006 | 0.029 | 0.024 |
| Ti | 2.030 | 1.910 | 0.979 | 0.944 | 0.061 |
| Al | 0.060 | 0.062 | 0.002 | 0.003 | 0.510 |
| Cr | 0.185 | 0.172 | 0.008 | 0.008 | 1.314 |
| Fe | 0.366 | 0.499 | 0.832 | 0.755 | 0.848 |
| Ni | 0.000 | - | 0.000 | 0.000 | 0.000 |
| Co | 0.001 | - | 0.000 | 0.000 | 0.000 |
| Mn | 0.007 | 0.005 | 0.014 | 0.010 | 0.012 |
| Mg | 0.106 | 0.106 | 0.140 | 0.236 | 0.219 |
| Ca | 0.164 | 0.148 | 0.019 | 0.014 | 0.008 |
| Na | 0.000 | - | 0.000 | 0.000 | 0.003 |
| K | 0.001 | - | 0.000 | 0.000 | 0.000 |
| P | 0.000 | - | 0.000 | 0.000 | 0.000 |
| Zr | 0.074 | 0.068 | 0.000 | 0.000 | 0.000 |
| *Charge* | *0.464* | *0.254* | *-0.020* | *-0.045* | *-0.011* |
| Ilm | | | 81.4 | 71.3 | |
| Geik | | | 13.8 | 22.3 | |
| Esk | | | 0.4 | 0.4 | |

As analyzed here, except * from Treiman and Drake (1983). Molar proportions are for ilmenite: Ilm = $FeTiO_3$; Geik = $MgTiO_3$; Esk = $Cr_2O_3$. *Charge* is total charge on mineral formula, assumes all Ti is +4; ideally *Charge* is zero.

.

Table 5. Comparison of Clast U Mineralogy to Magnesian Suite Noritic Lithologies and Magnesian Feldspathic Granulites & Impact melts

| Character | Clast U | **Mg-suite Norite** | *Mg-suite Gabbronorite* | Magnesian Feldspathic Granulite, Impact Melt |
|---|---|---|---|---|
| Pyroxene | **LoCa > HiCa** | **LoCa > HiCa** | *HiCa > LoCa* | LoCa > HiCa |
| FeO/MgO | **Lower** | **Lower** | *Higher* | Lower |
| $Cr_2O_3$ | *Lower* | **Higher** | *Lower* | Higher or Lower |
| Plagioclase | **An89-97** | **> An88** | *< An90* | An95-97 |
| | | | | |
| Minor Minerals | | | | |
| Kspar | Absent | **Present** | *Present* | Absent |
| Ca-phosphate | Present | **Present, more** | *Present, less* | Rare |
| Cr-Al-spinel | **Cr-rich** | **Cr-rich** | *Al-rich* | Cr-rich and Al-rich |
| Ilmenite | **Present** | **Present** | *Common* | Rare |
| Armalcolite | **Present** | **Present** | *Rare* | Absent |
| Rutile | **Present** | **Present** | *Rare* | Absent |
| Zircon | *Absent* | **Present** | *Absent* | Absent |
| Zr-Nb mins | **Zr-armalcolite** | **Present** | *Absent* | Absent |

Criteria for classification from James and Flohr (1983) and Norman et al. (1995), see Figure 8. Characteristics of magnesian-norites in boldface, those of magnesian gabbronorites in italics. Characteristics of magnesian feldspathic granulites and impactites from Takeda et al. (2006); Treiman et al. (2010). Characteristics of Clast U that fit both or neither magnesian norite nor gabbronorite shown in normal typeface.

Table 3. EMP Analyses of Olivine for Trace Elements

| Set/Point | 1 / 3 | 1 / 4 | 1 / 5 | 1 / 6 | 1 / 7 | 1 / 8 | 1 / 9 | 1 / 10 | 1 / 11 |
|---|---|---|---|---|---|---|---|---|---|
| $SiO_2$ | 39.14 | 40.09 | 40.87 | 40.13 | 38.93 | 38.89 | 39.00 | 38.94 | 38.39 |
| $TiO_2$ | 0.04 | 0.04 | 0.04 | 0.03 | 0.04 | 0.06 | 0.06 | 0.05 | 0.05 |
| $Al_2O_3$ | 0.79 | 0.91 | 0.88 | 0.26 | 0.15 | 0.21 | 0.29 | 0.70 | 0.87 |
| $Cr_2O_3$ | 0.05 | 0.04 | 0.05 | 0.04 | 0.05 | 0.05 | 0.05 | 0.05 | 0.05 |
| FeO | 15.88 | 15.88 | 16.26 | 16.95 | 16.26 | 16.08 | 16.06 | 16.05 | 15.82 |
| MnO | 0.21 | 0.22 | 0.22 | 0.21 | 0.23 | 0.23 | 0.22 | 0.22 | 0.21 |
| MgO | 43.33 | 42.96 | 41.62 | 42.47 | 43.90 | 43.75 | 43.61 | 43.53 | 42.75 |
| CaO | 0.37 | 0.41 | 0.37 | 0.15 | 0.09 | 0.09 | 0.11 | 0.22 | 0.27 |
| Total | 99.82 | 100.56 | 100.30 | 100.26 | 99.66 | 99.36 | 99.40 | 99.77 | 98.42 |
| Co ppm | bdl | bdl | bdl | bdl | bdl | bdl | bdl | bdl | bdl |
| Ni ppm | 58.6 | 27.1 | 41.0 | 62.9 | 53.4 | 71.5 | 74.3 | 57.4 | 72.1 |
| Si | 0.990 | 1.009 | 1.037 | 1.018 | 0.986 | 0.987 | 0.990 | 0.985 | 0.985 |
| Ti | 0.001 | 0.001 | 0.001 | 0.001 | 0.001 | 0.001 | 0.001 | 0.001 | 0.001 |
| Al | 0.024 | 0.027 | 0.026 | 0.008 | 0.005 | 0.006 | 0.009 | 0.021 | 0.026 |
| Cr | 0.001 | 0.001 | 0.001 | 0.001 | 0.001 | 0.001 | 0.001 | 0.001 | 0.001 |
| Fe | 0.336 | 0.334 | 0.345 | 0.359 | 0.344 | 0.341 | 0.341 | 0.340 | 0.339 |
| Mn | 0.005 | 0.005 | 0.005 | 0.005 | 0.005 | 0.005 | 0.005 | 0.005 | 0.005 |
| Mg | 1.634 | 1.612 | 1.575 | 1.605 | 1.657 | 1.656 | 1.651 | 1.642 | 1.635 |
| Ca | 0.010 | 0.011 | 0.010 | 0.004 | 0.002 | 0.002 | 0.003 | 0.006 | 0.008 |
| Fo | 83 | 83 | 82 | 82 | 83 | 83 | 83 | 83 | 83 |
| Fe/Mn | 73 | 71 | 75 | 78 | 70 | 69 | 73 | 71 | 76 |
| *Chg* | 0.006 | 0.048 | 0.103 | 0.045 | -0.022 | -0.016 | -0.008 | -0.006 | -0.001 |

| Set/Point | 1 / 12 | 1 / 13 | 1 / 14 | 1 / 15 | 2 / 2 | 2 / 3 | 3 / 2 | 3 / 3 | average |
|---|---|---|---|---|---|---|---|---|---|
| $SiO_2$ | 38.70 | 38.74 | 39.01 | 39.48 | 38.62 | 38.57 | 38.95 | 38.96 | 39.14 |
| $TiO_2$ | 0.05 | 0.05 | 0.05 | 0.06 | 0.04 | 0.04 | 0.04 | 0.05 | 0.04 |
| $Al_2O_3$ | 0.87 | 0.23 | 0.17 | 0.89 | 0.26 | 0.18 | 0.56 | 0.58 | 0.52 |
| $Cr_2O_3$ | 0.05 | 0.05 | 0.09 | 0.18 | 0.06 | 0.05 | 0.06 | 0.05 | 0.06 |
| FeO | 15.89 | 16.08 | 16.16 | 15.46 | 16.08 | 16.16 | 15.34 | 15.44 | 15.99 |
| MnO | 0.23 | 0.23 | 0.22 | 0.24 | 0.23 | 0.23 | 0.21 | 0.22 | 0.22 |
| MgO | 42.78 | 43.41 | 43.55 | 42.05 | 43.10 | 43.13 | 43.90 | 43.88 | 43.16 |
| CaO | 0.32 | 0.09 | 0.08 | 0.41 | 0.09 | 0.11 | 0.33 | 0.29 | 0.22 |
| Total | 98.89 | 98.88 | 99.33 | 98.77 | 98.48 | 98.47 | 99.41 | 99.48 | 99.37 |
| Co ppm | bdl | bdl | bdl | bdl | bdl | bdl | bdl | bdl | bdl |
| Ni ppm | 37.2 | 41.9 | 45.8 | 14.0 | 32.5 | 48.8 | 56.1 | 65.4 | 51±33 |
| Si | 0.989 | 0.989 | 0.992 | 1.013 | 0.990 | 0.989 | 0.986 | 0.986 | 0.995 |
| Ti | 0.001 | 0.001 | 0.001 | 0.001 | 0.001 | 0.001 | 0.001 | 0.001 | 0.001 |
| Al | 0.026 | 0.007 | 0.005 | 0.027 | 0.008 | 0.006 | 0.017 | 0.017 | 0.016 |
| Cr | 0.001 | 0.001 | 0.002 | 0.004 | 0.001 | 0.001 | 0.001 | 0.001 | 0.001 |
| Fe | 0.340 | 0.343 | 0.344 | 0.332 | 0.345 | 0.347 | 0.325 | 0.327 | 0.340 |
| Mn | 0.005 | 0.005 | 0.005 | 0.005 | 0.005 | 0.005 | 0.005 | 0.005 | 0.005 |
| Mg | 1.630 | 1.652 | 1.650 | 1.608 | 1.648 | 1.649 | 1.657 | 1.655 | 1.636 |
| Ca | 0.009 | 0.002 | 0.002 | 0.011 | 0.003 | 0.003 | 0.009 | 0.008 | 0.006 |
| Fo | 83 | 83 | 83 | 83 | 83 | 83 | 84 | 84 | 83 |
| Fe/Mn | 68 | 68 | 73 | 65 | 70 | 71 | 71 | 71 | 71 |
| *Chg* | 0.007 | -0.013 | -0.008 | 0.058 | -0.009 | -0.014 | -0.008 | -0.008 | 0.009 |

Analytical conditions described in text. All analyses for Co are below the 3σ detection limit of 40 ppm (bdl). Individual analyses for Ni have 3σ detection limits of ~40 ppm. Average is of all 17 points; uncertainty on Ni is 2σ of the population. For the average analysis, the 3σ detection limit for Ni is ~10 ppm. Normalizations to three cations; Fo is molar Mg/(Mg+Fe); Fe/Mn is molar; *Chg* is charge on normalized formula of 3 cations and 4 $O^{2-}$; ideally, each analysis should be charge-balanced with *Chg* = 0.

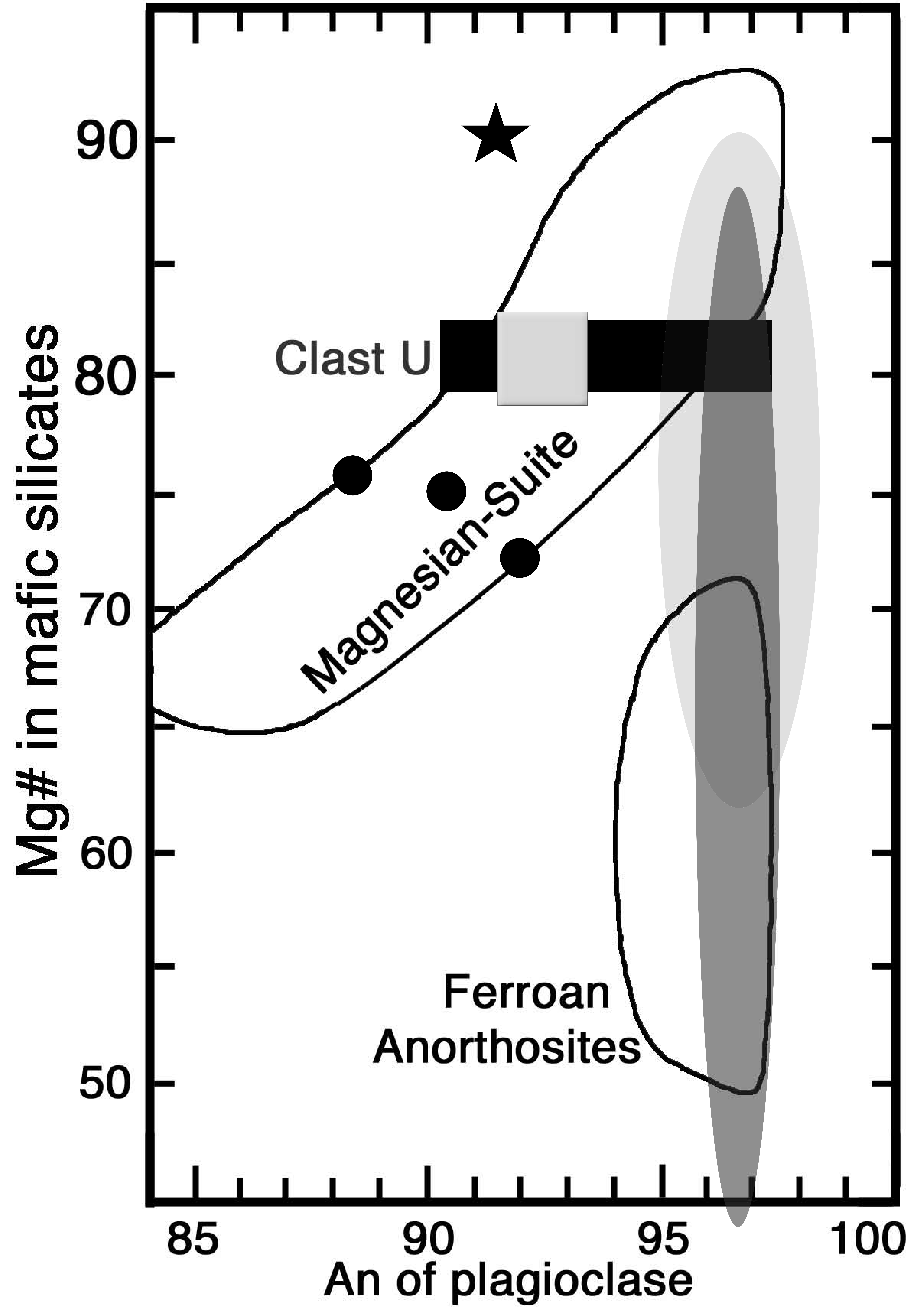

Mg# in mafic silicates
90
80
70
60
50
Clast U
Magnesian-Suite
Ferroan
Anorthosites
85
90
95
100
An of plagioclase


1 mm

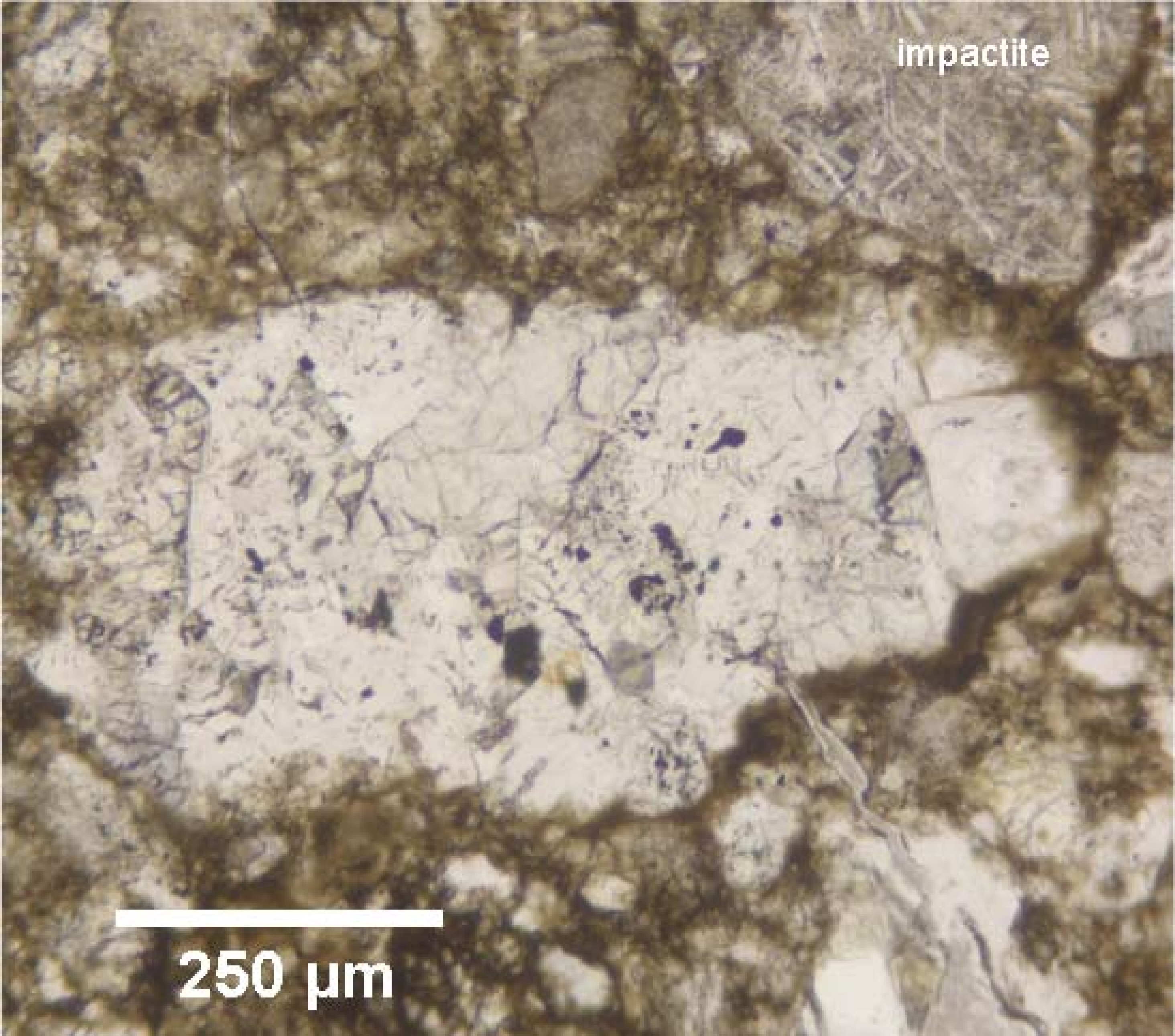
impactite
250 µm

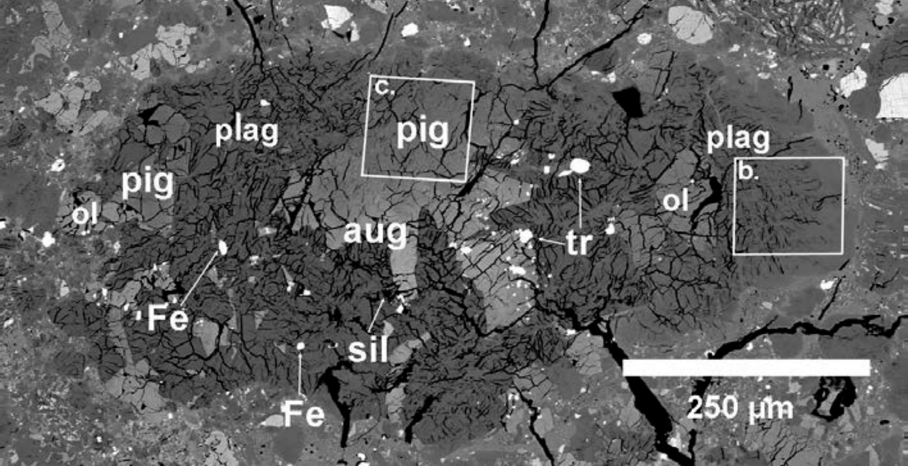

c.
pig
plag
plag
b.
pig
ol
ol
aug
tr
Fe
sil
Fe
250 µm

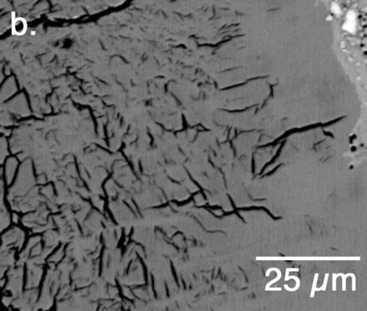
b.
25 μm

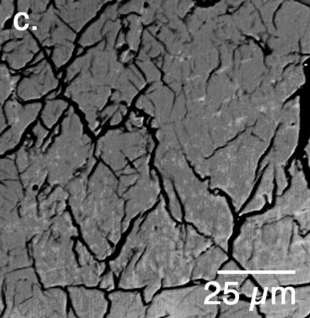
c.
25 μm

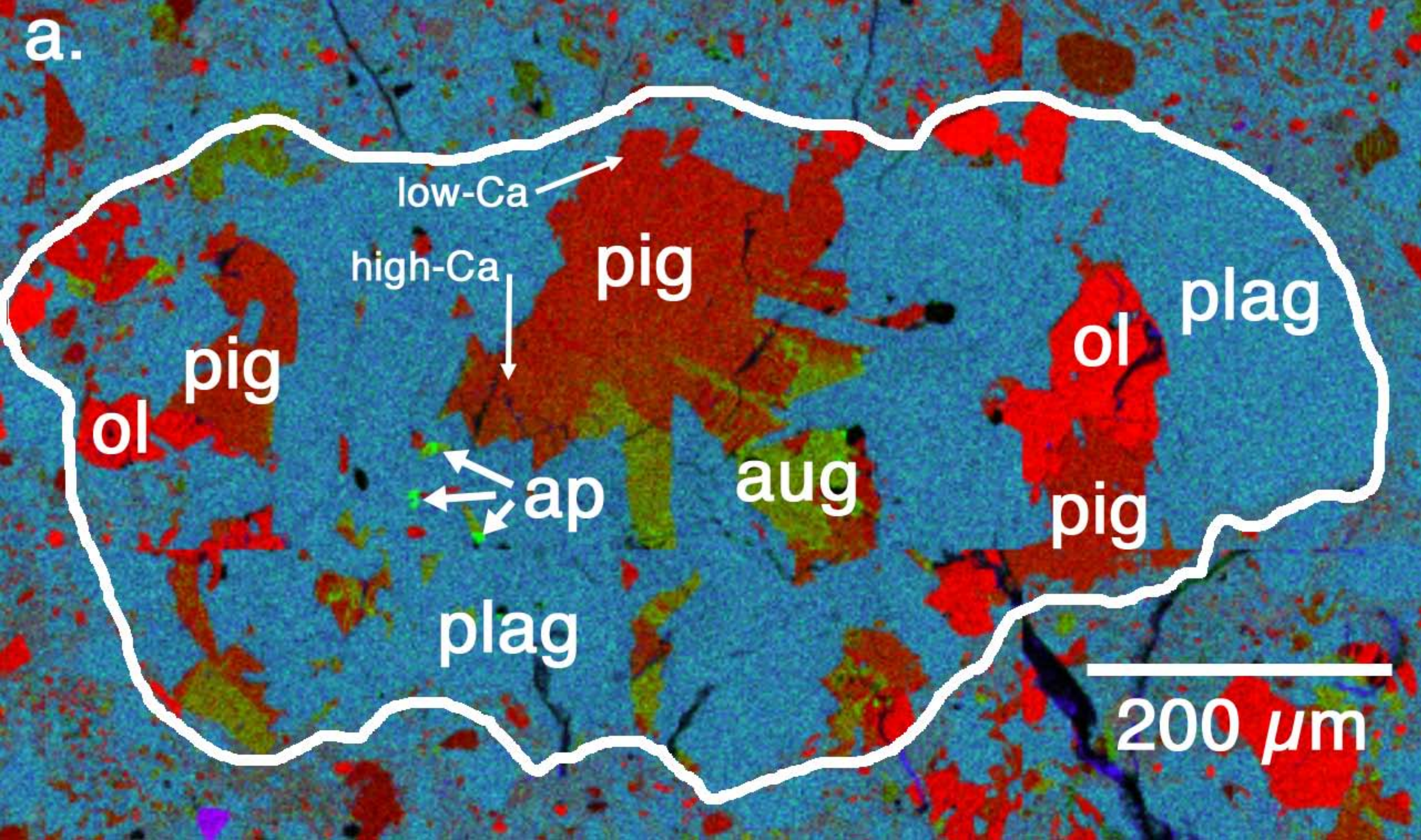
a.
low-Ca
high-Ca
pig
pig
ol
ol
plag
pig
aug
ap
plag
200 μm

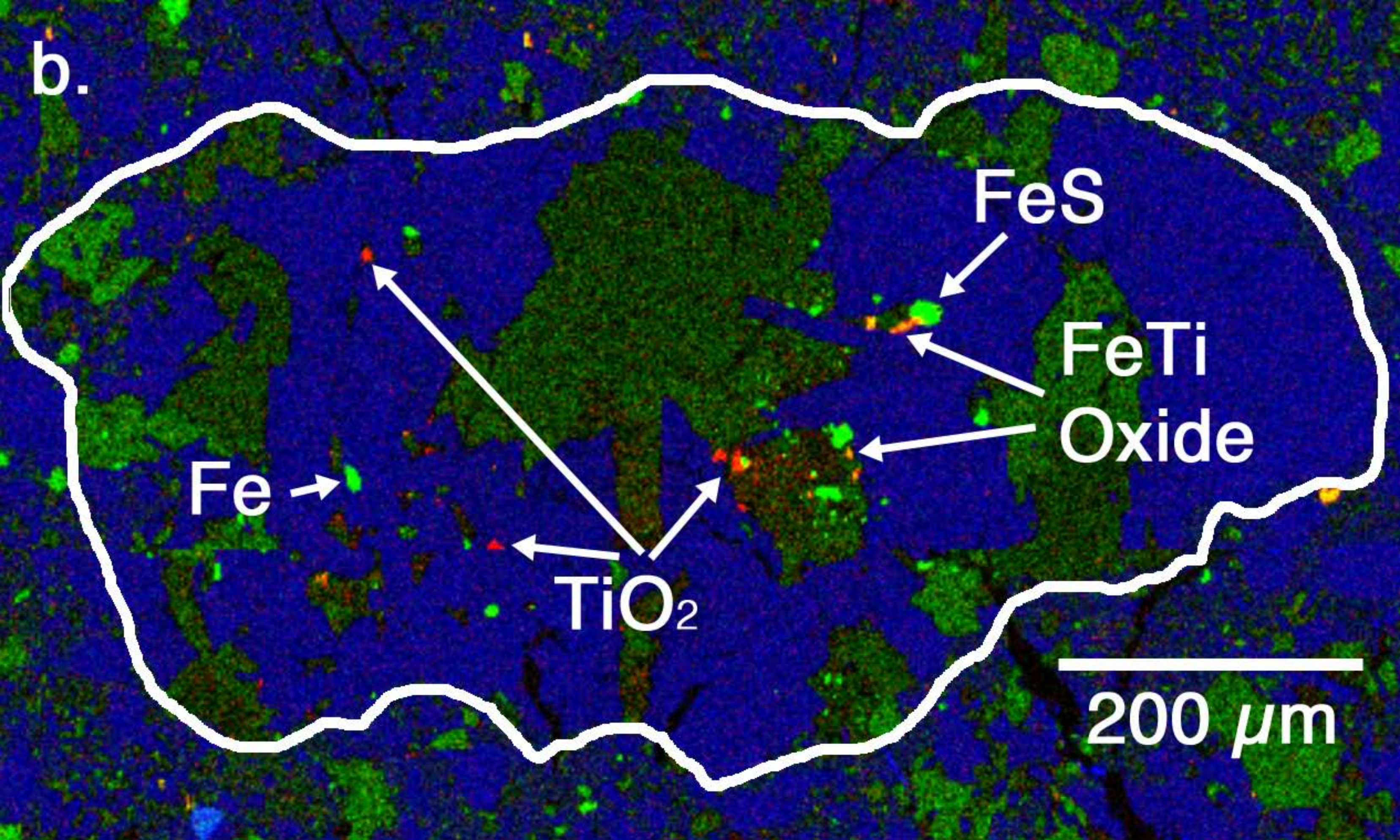

b.
FeS
FeTi
Oxide
Fe
TiO2
200 μm

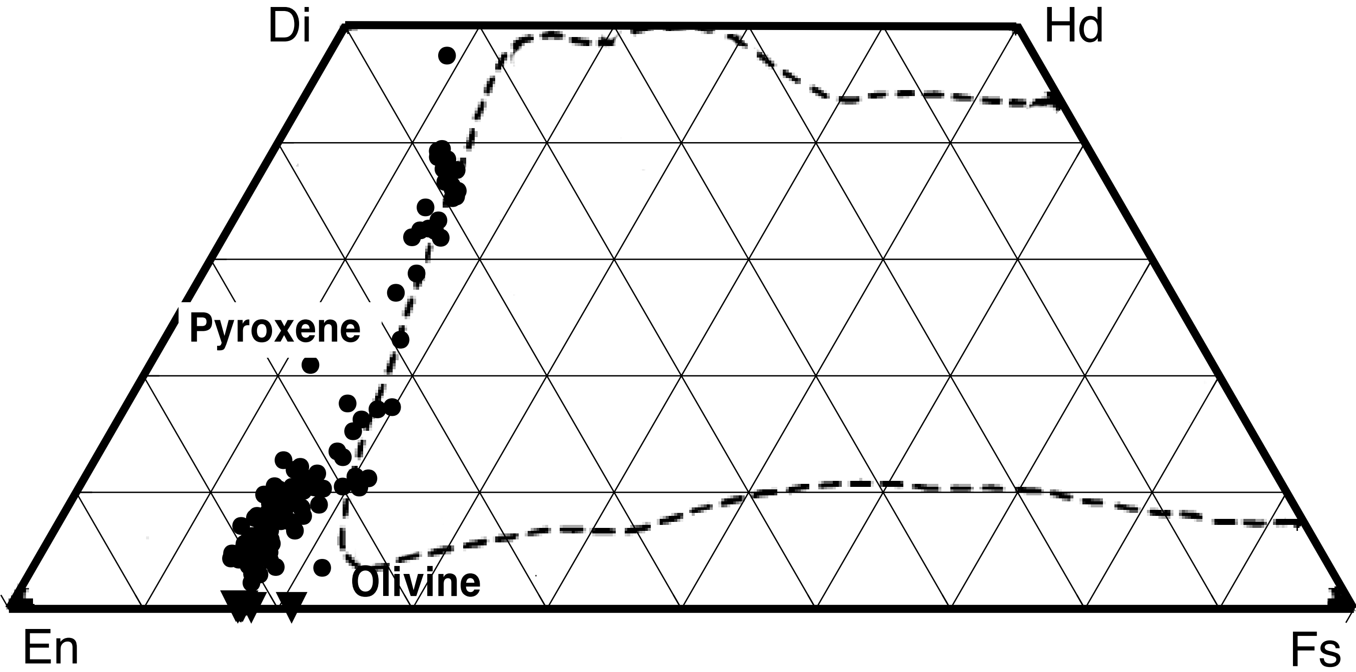
Di
Hd
Pyroxene
Olivine
En
Fs

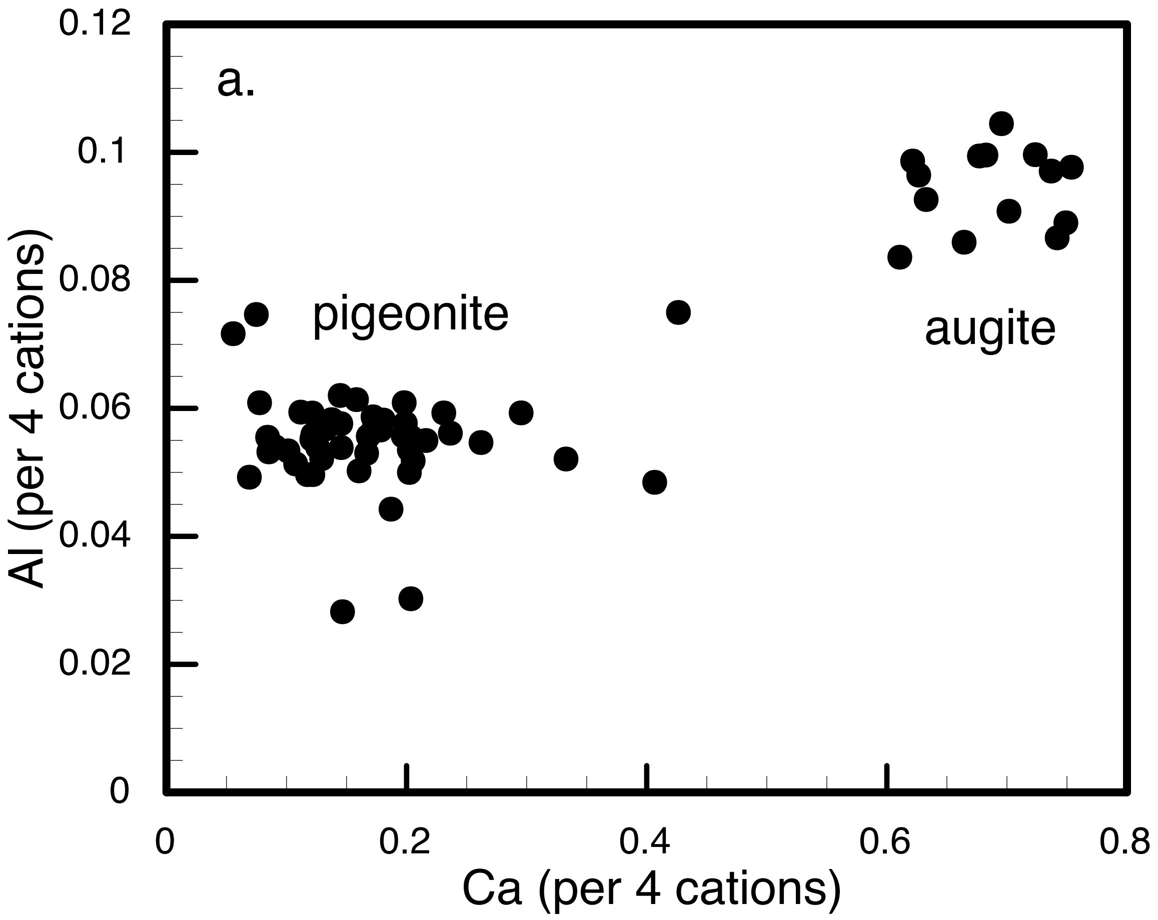
a.
pigeonite
augite
Al (per 4 cations)
Ca (per 4 cations)
0
0.02
0.04
0.06
0.08
0.1
0.12
0
0.2
0.4
0.6
0.8

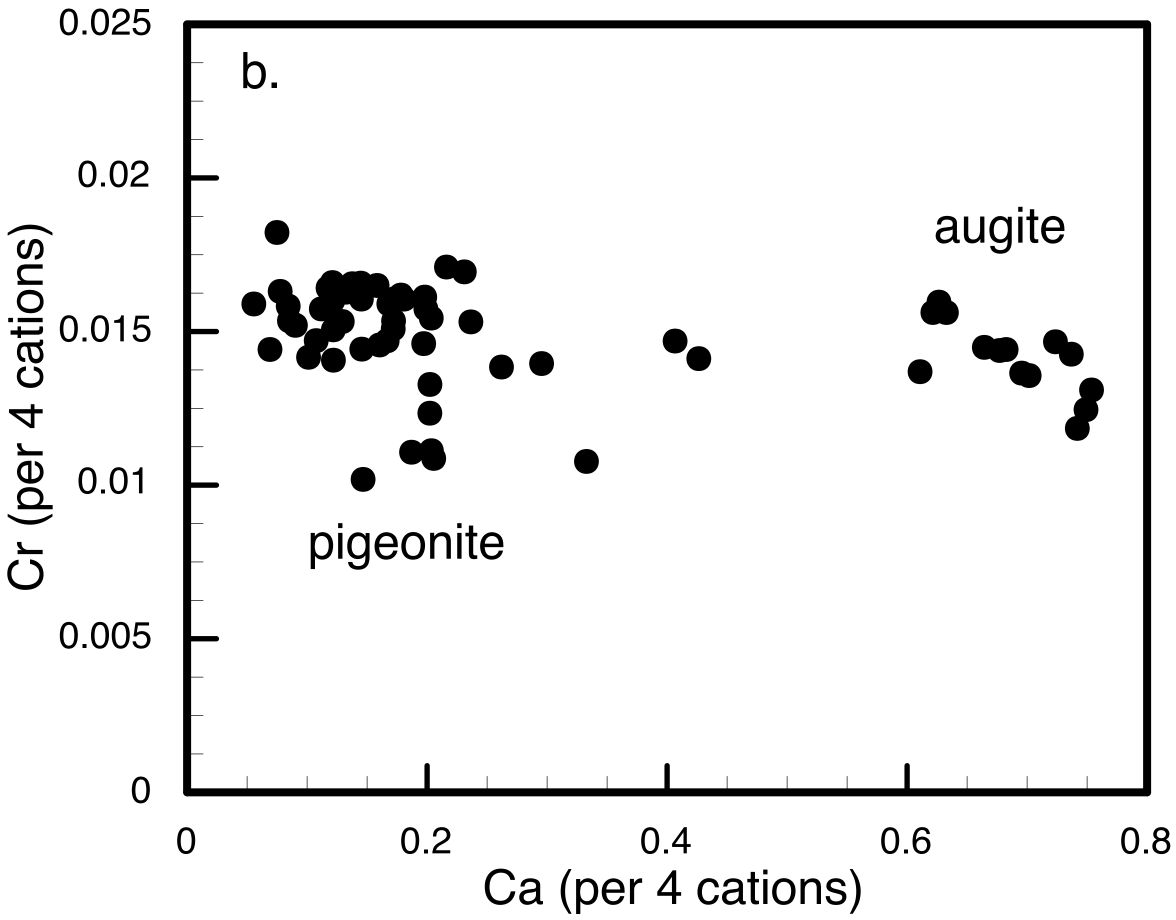

b.
augite
pigeonite
0.025
0.02
0.015
0.01
0.005
0
Cr (per 4 cations)
0
0.2
0.4
0.6
0.8
Ca (per 4 cations)

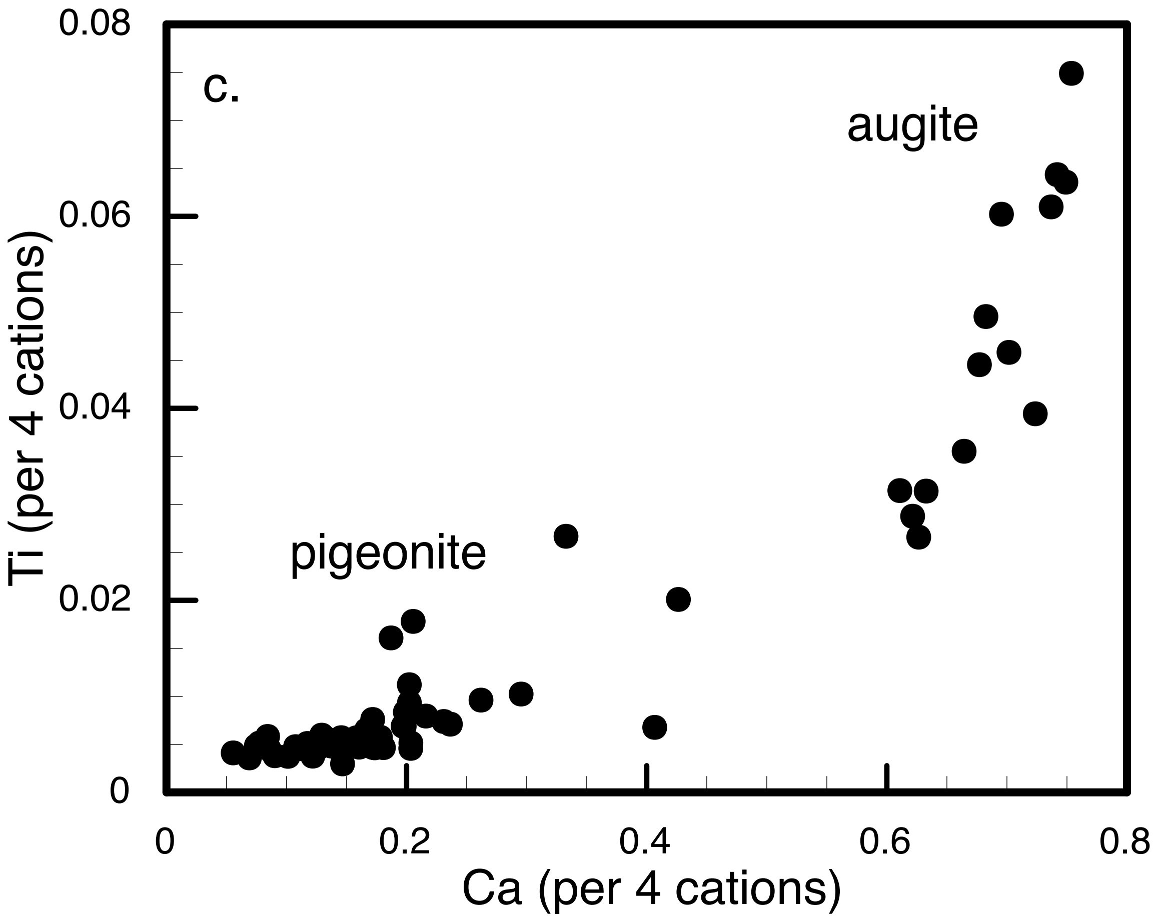
c.
augite
pigeonite
Ti (per 4 cations)
Ca (per 4 cations)
0
0.02
0.04
0.06
0.08
0.2
0.4
0.6
0.8

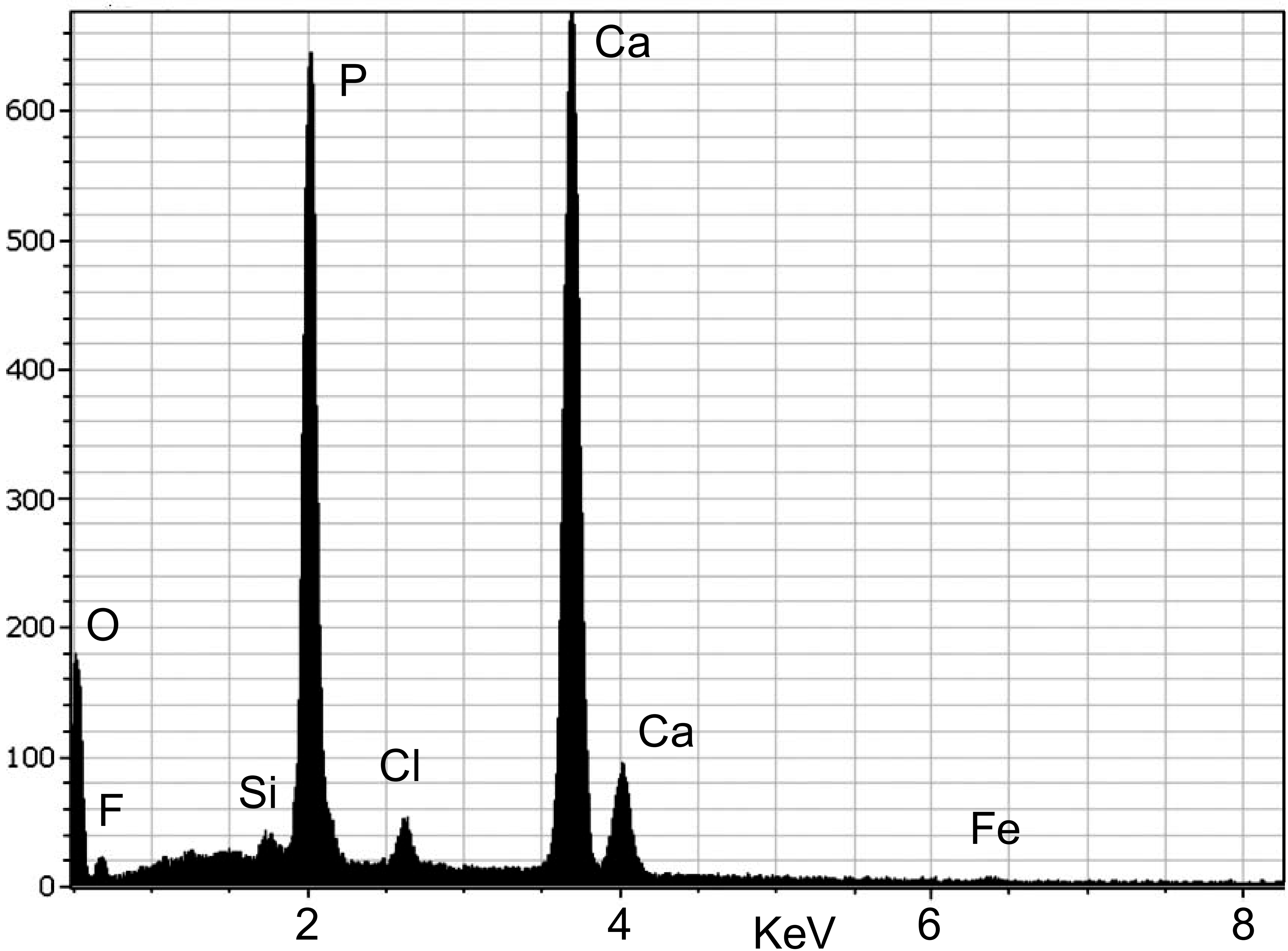
Ca
P
O
Ca
Cl
Si
F
Fe
600
500
400
300
200
100
0
2
4
KeV
6
8

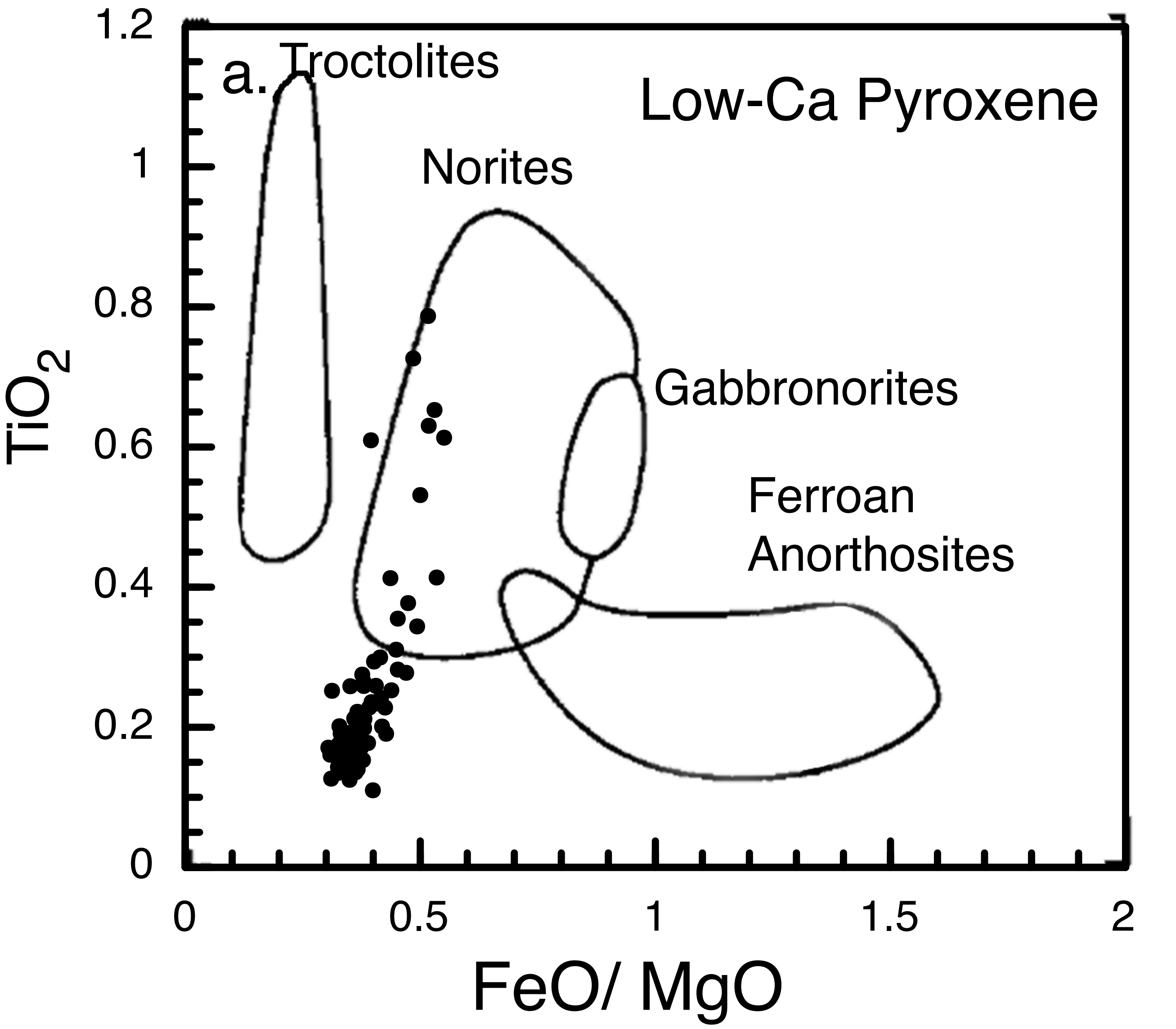

a. Troctolites
Low-Ca Pyroxene
Norites
Gabbronorites
Ferroan
Anorthosites
TiO2
FeO/ MgO
1.2
1
0.8
0.6
0.4
0.2
0
0
0.5
1
1.5
2

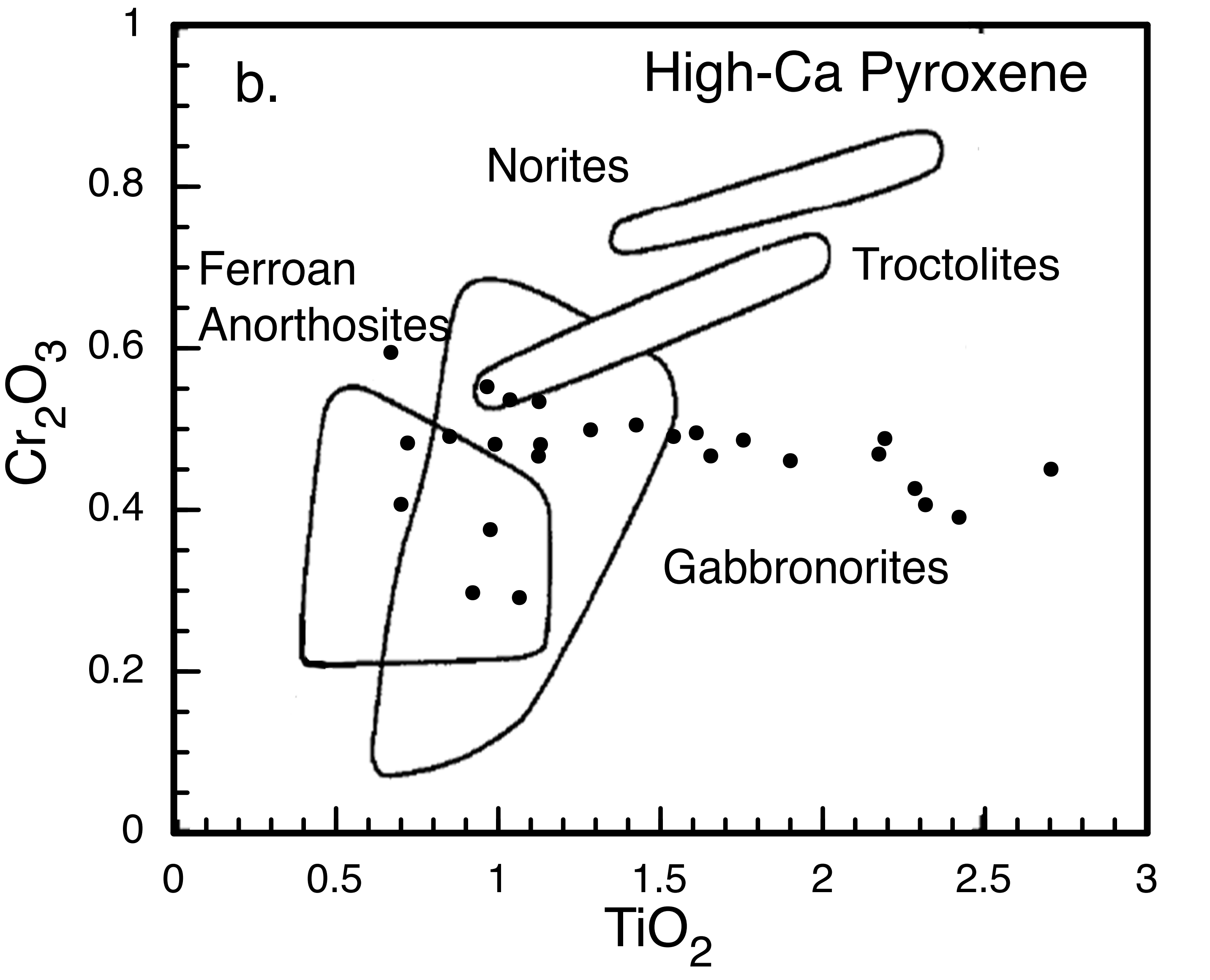
b.
High-Ca Pyroxene
Norites
Ferroan
Anorthosites
Troctolites
Gabbronorites
Cr2O3
TiO2
0
0.2
0.4
0.6
0.8
1
0
0.5
1
1.5
2
2.5
3

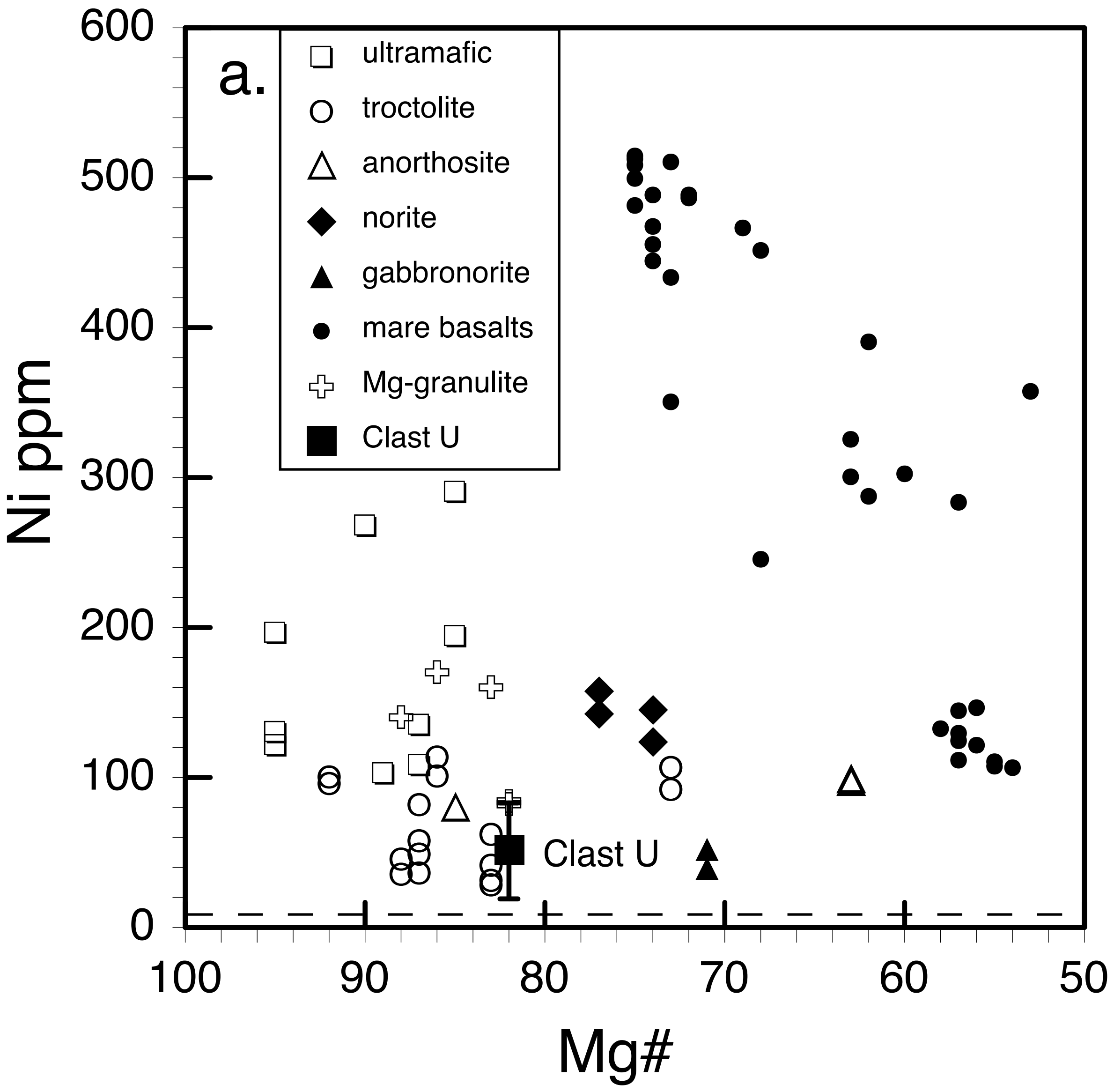
a.
ultramafic
troctolite
anorthosite
norite
gabbronorite
mare basalts
Mg-granulite
Clast U
Clast U
Ni ppm
Mg#
600
500
400
300
200
100
0
100
90
80
70
60
50

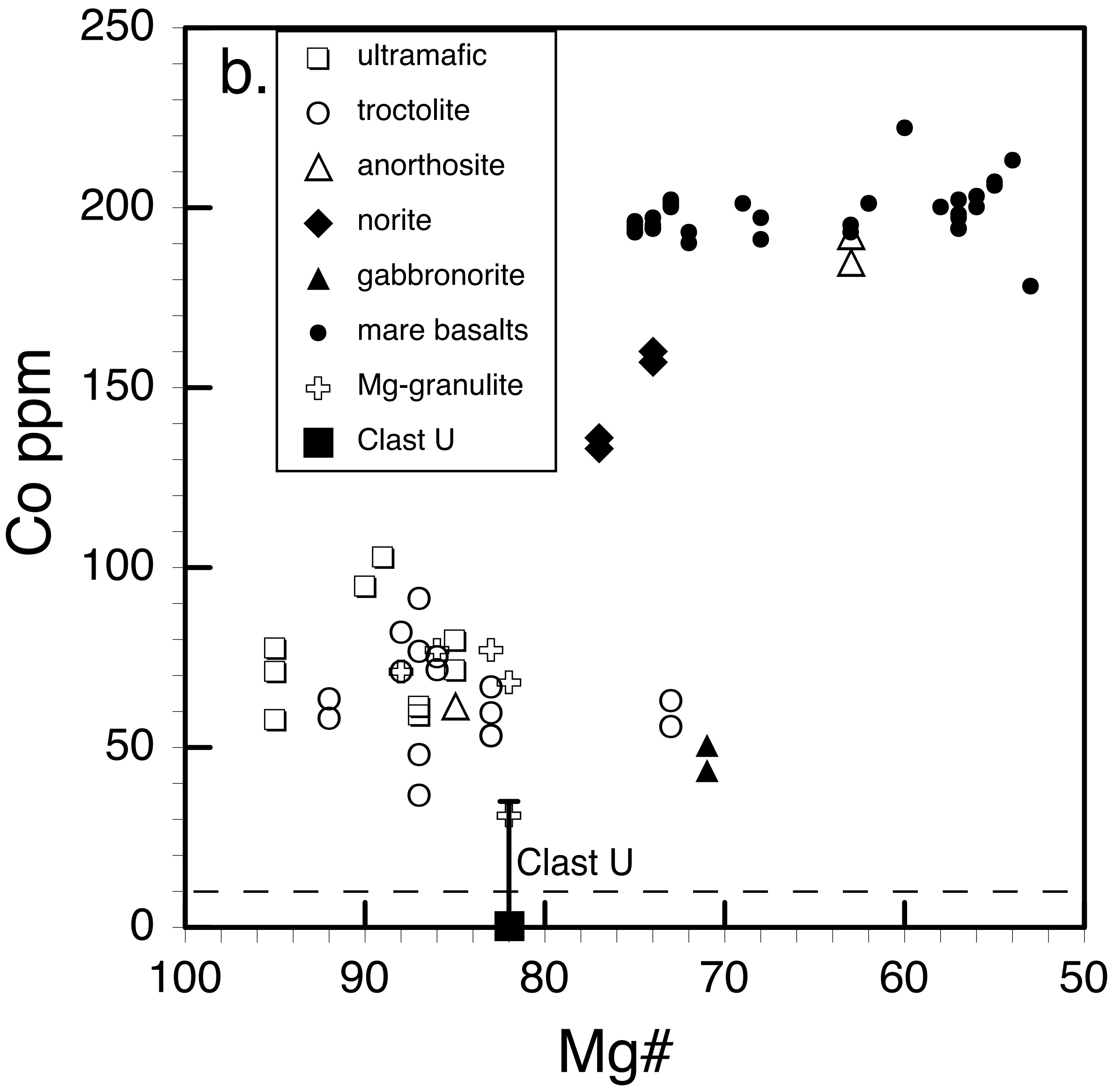
b.
ultramafic
troctolite
anorthosite
norite
gabbronorite
mare basalts
Mg-granulite
Clast U
Clast U
Co ppm
Mg#
250
200
150
100
50
0
100
90
80
70
60
50